

DIRECT OBSERVATION OF BALLISTIC ANDREEV REFLECTION

T. M. Klapwijk^{a,b*}, *S. A. Ryabchun*^{b,c}

^a*Kavli Institute of NanoScience, Faculty of Applied Sciences, Delft University of Technology
2628, CJ Delft, The Netherlands*

^b*Laboratory for Quantum Limited Devices, Physics Department, Moscow State Pedagogical University
119992, Moscow, Russia*

^c*Moscow Institute of Electronics and Mathematics, National Research University Higher School of Economics
109028, Moscow, Russia*

Received June 9, 2014

An overview is presented of experiments on ballistic electrical transport in inhomogeneous superconducting systems which are controlled by the process of Andreev reflection. The initial experiments based on the coexistence of a normal phase and a superconducting phase in the intermediate state led to the concept itself. It was followed by a focus on geometrically inhomogeneous systems like point contacts, which provided a very clear manifestation of the energy and direction dependence of the Andreev reflection process. The point contacts have recently evolved towards the atomic scale owing to the use of mechanical break-junctions, revealing a very detailed dependence of Andreev reflection on the macroscopic phase of the superconducting state. In present-day research, the superconducting inhomogeneity is constructed by clean room technology and combines superconducting materials, for example, with low-dimensional materials and topological insulators. Alternatively, the superconductor is combined with nano-objects, such as graphene, carbon nanotubes, or semiconducting nanowires. Each of these “inhomogeneous systems” provides a very interesting range of properties, all rooted in some manifestation of Andreev reflection.

Contribution for the JETP special issue in honor of A. F. Andreev's 75th birthday

DOI: 10.7868/S0044451014120013

1. INTRODUCTION

The 50-year-old concept of Andreev reflection [1], published in May 1964, arose originally in the context of ballistic transport in inhomogeneous crystalline materials with parts in the superconducting phase intermixed with parts in the normal phase. The difference between the electrical and thermal conductivities, already observed in the early 1950s by Mendelsohn and Olsen [2], and Hulm [3] was not resolved by the 1959 microscopic theory of the thermal conductivity by Bardeen et al. [4]. Subsequent experimental work by Zavaritskii [5] in 1960, and by Strässler and Wyder [6] in 1963 led Andreev to the analysis of electron transport at the interface between the normal and the superconducting phase in the same crystal. He identified the unique process of the conversion of an electron

into a hole which retraces the path of the incident electron, accompanied by the simultaneous process of a charge of $2e$ being carried away by the superconducting condensate. This process facilitated charge transport but it did not allow for energy transport and the observed thermal boundary resistance was a natural consequence [1, 7].

An interface between a normal metal and a superconductor is an example of an inhomogeneous superconducting system. Since the early 1950s, the natural framework for dealing with a position-dependent superconducting order parameter was provided by the Ginzburg–Landau theory [8]. The original BCS theory [9, 10] assumed a uniform superconducting state. By developing a formulation in 1958 of the microscopic theory [11], which allows for spatial variations, Gorkov [12] showed in 1959 that the Ginzburg–Landau theory can be derived from the microscopic theory. The Ginzburg–Landau theory is only valid close to the critical temperature T_c , whereas the difference in thermal

*E-mail: t.m.klapwijk@tudelft.nl

and electrical conductivities was primarily manifest at temperatures much lower than T_c . A conceptual framework for inhomogeneous superconductors was needed, which included the spectral properties of the superconducting state, which is available in the original Gorkov theory [11]. The Bogoliubov–De Gennes equations, which are now commonly used, are a limit case of these Gorkov equations, suitable for treating ballistic transport.

From the experimental point of view, another very important step was taken almost simultaneously in 1965 by Sharvin [13] by the invention of mechanically constructed metallic point contacts. This allowed the study of electrical transport between two dissimilar materials, with electrical transport governed by classically ballistic electrons. The application of this concept of ballistic transport to normal-metal–superconductor contacts provided the framework, introduced by Blonder et al. [14], to measure the energy dependence of the Andreev scattering process very directly. The Sharvin point contacts also stimulated a new approach to the description of electrical transport on the nanoscale level by using the scattering matrix approach, introduced already in 1957 by Landauer [15] and generalized and applied to phase-coherent normal transport in nanoscale objects by Büttiker in 1985 [16]. Rather than relying on a general theory for inhomogeneous systems, it focuses on simplified experimental systems in which the phase-coherent transport problem can be split into three pieces. It selects the class of problems in which two equilibrium reservoirs can be defined, usually at a different chemical potentials or temperatures, which serve as emitters or absorbers of quantum particles and a scattering region in which the interesting physical processes occur and which can be characterized by a scattering matrix with certain symmetry properties.

The experimental progress in constructing nano-objects with the clean room technology, now universally available, has led to many experiments based on nano-objects connected to superconducting rather than normal-metal reservoirs. This leads to a large variety of objects and observations in which the challenge is to discover new phenomena and at the same time establish through transport experiments what has actually been made in the clean room. In some cases, the general theory of inhomogeneous nonequilibrium superconductivity is used to interpret these specific cases. At the same time, the perceived unique nature of these nano-objects has led to an application of the scattering-matrix approach, in which the superconducting contacts serve as equilibrium reservoirs that communicate with the scattering region through the Andreev reflection pro-

cess. An experimental challenge is to determine which framework is appropriate for the actual nano-objects emerging from the clean room and where theoretical innovation is needed.

In what follows, we attempt to summarize the developments in the subject over the past 50 years. The focus is on experimental observations, which provide a direct demonstration related to ballistic Andreev reflection. The main attention is paid to the demonstration of the reversal of direction, as well as of the charge, and the spectroscopically important dependence on energy. Furthermore, a third important aspect is the dependence on the macroscopic quantum phase, which manifests itself when more than one superconductor is used. It leads to the concept of Andreev bound states, which carry the Josephson current. Since the field has become large, a further selection was applied by focusing on experiments that are sufficiently well-defined, such that a quantitative description turns out to be possible. Needless to say, many experiments are not included, in particular those in which diffusive scattering is the dominant ingredient. The section headings give an indication of the subject. They are supplemented with the dates in which, in our view, the most significant developments for this subject took place.

2. INHOMOGENEOUS SUPERCONDUCTIVITY CLOSE TO T_c : 1950–1957

After the discovery of superconductivity by observing zero resistance by Kamerlingh Onnes in 1911, it took until 1933 for a second fundamental property to be identified by Meissner and Ochsenfeld, and called perfect diamagnetism. An early explanation was provided by Fritz and Heinz London in 1935 by a modification of the Maxwell equations inside a superconducting material. It was known that these properties were very nicely observed in pure crystals of tin, aluminium, and mercury. However, it was also known that many superconducting alloys did not obey these basic relations. In particular, perfect diamagnetism was not observed although the material provided zero resistance. Apparently, magnetic flux was not completely excluded and the magnetization curve was not reversible but showed clearly hysteretic effects. The first theory capable of handling inhomogeneous systems was the Ginzburg–Landau theory, introduced in 1950. It was used by Abrikosov in 1957 to analyze what would happen with a superconductor if the magnetic penetration depth λ_L known from the London theory exceeded another char-

acteristic length ξ , now called the Ginzburg–Landau coherence length.

By minimizing the expression for the free energy in a volume in which the order parameter can vary with position, we find the two celebrated Ginzburg–Landau (GL) expressions

$$\frac{1}{2m^*} \left[-i\hbar\nabla - \frac{e^*A}{c} \right]^2 \psi + \alpha\psi + \beta|\psi|^2\psi = 0 \quad (1)$$

and

$$j = \frac{e^*\hbar}{2im^*} (\psi^*\nabla\psi - \psi\nabla\psi^*) - \frac{e^{*2}}{m^*c} \psi^*\psi A. \quad (2)$$

These two equations allow calculating the order parameter as a function of position in the presence of a magnetic field, including the distribution of the current. The magnetic field H is the locally present field strength. And, of course, it is assumed that the order parameter ψ is complex with a phase ϕ , which can also be position dependent.

The most ideal inhomogeneous system is one in which we have a clearly defined boundary between a piece of atomic matter in the superconducting state and a piece of the same atomic matter in the normal state. In such a system, no barrier would be encountered for normal electronic transport, because the material is uniform in its atomic arrangement. Obviously, this is not the case in the many nano-devices studied today, which consist of different materials with different atomic arrangements. This nonuniformity in the atomic sense, which goes beyond the superconducting properties, is an experimental nuisance. However, it contributes strongly to the interplay between elastic and Andreev scattering. Below, we sketch two cases in which this complexity is absent.

2.1. Inhomogeneous system created with an applied magnetic field: intermediate state

In type-II superconductors, discovered by Abrikosov, λ is much larger than ξ and quantized vortices are the dominant inhomogeneous state, with their own interesting microscopic properties. In the other limit, $\lambda \ll \xi$, in the presence of a magnetic field, the material breaks up in lamellae of alternating superconducting and normal phase. One of the attractive features of this intermediate state in type-I superconductors is that it provides a system with uncompromised interfaces between a normal state and a superconducting state. In the same material with the same atomic constituents, we then have a domain with electrons in the normal

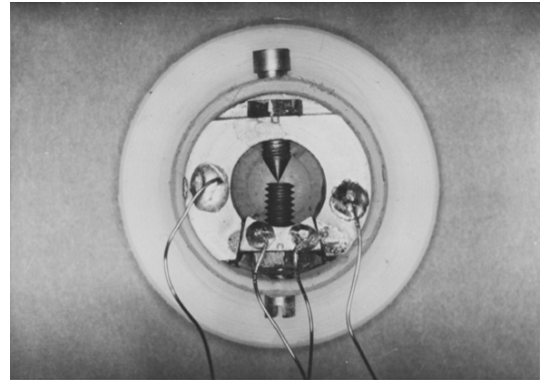


Fig.1. Superconducting point contact made of a pointed niobium screw touching a niobium anvil, both in a yoke of superconducting material, separated by a thin layer of glass with the same thermal expansion coefficient as that of niobium. From the perspective of the electrons, the actual contact is formed by a metallic path punching through the surface oxide

state and a domain with electrons in the superconducting state. The price to be paid is that the normal state occurs in the presence of a magnetic field. However, the normal state is hardly affected by the presence of this magnetic field.

For a material such as tin or aluminium, a single crystal can be grown with an elastic scattering length of the order of millimeters. The ratio of the resistance at room temperature compared to the one at low temperatures can be in the range of several 10000s. The crystals can have a high degree of purity with an impurity resistance very low compared to the resistance caused by electron–phonon scattering. These crystals have been used extensively to study transport properties. The electrical resistance in this intermediate state is very well understood as being due to the resistivity of the normal state multiplied by the thickness of the normal slabs and their number. The difficulty was that the thermal resistance did not behave in the same way. It appeared as if there was a thermal boundary resistance present, which increased with lowering the temperature. This difference was the starting point for the concept of Andreev reflections.

2.2. Constriction-type inhomogeneity

Another example of an inhomogeneous system is a constriction-type Josephson weak link [17]. We consider two massive volumes of a superconductor, which are only linked to each other at one point by a short and narrow piece of the same superconductor (see Fig. 1).

In the absence of a magnetic field and a current, the superconducting order parameter ψ is everywhere the same. If a current is applied, the current density is low in the banks of the point contact and high in the neck, where a strong gradient of ψ is present. Aslamazov and Larkin [18] have analyzed this case, starting with the observation that the dominant term in Eq. (1) is the second-derivative term,

$$\nabla^2 \psi = 0, \quad (3)$$

which has to be solved together with Eq. (2). The inhomogeneity is in this case due to the different cross sections, which enforce a strong difference in the current density.

The current can be expressed using the second Ginzburg–Landau equation (Eq. (2)), leading to

$$J_s = C |\psi_1| |\psi_2| \sin(\phi_1 - \phi_2). \quad (4)$$

This simple derivation has shown in an elegant way that the characteristic $\sin \phi$ dependence of the Josephson effect emerges quite generally, close to T_c , for both dirty and clean superconductors. The important assumption is that two equilibrium reservoirs are connected by a weak link, which allows reducing the problem to solving Eq. (3), in this case under the assumption that the Ginzburg–Landau equations can be applied, valid for small values of the order parameter ($\Delta \ll k_B T$). It is customary to assume that in the presence of a voltage, the supercurrent has a parallel current given by Ohm’s law, $I_n = V/R$, with R being a voltage-independent resistance, without any information about the microscopic superconducting properties. In subsequent research, it has become clear that the voltage dependence of the “normal” transport, i. e., the nonlinearity of the resistor, is a rich source of information about the microscopic properties. In experiments, it is unavoidable, given the way the point contacts are made, that there is a possibility of enhanced elastic scattering at the constriction itself, unlike in the previous case of the intermediate state.

3. INHOMOGENEOUS SYSTEMS FAR BELOW T_c : 1963–1966

The original microscopic theory of superconductivity considers a uniform system. Within this framework, the electronic thermal conductance was calculated by Bardeen, Rickayzen, and Tewordt [4], showing an exponential decay of the electronic contribution to thermal conductivity, in line with the reduction of the quasi-particle density. Given the examples above, the challenge is to deal also with inhomogeneous superconducting systems in the limit $\Delta \gg k_B T$. In the opposite limit

$\Delta \ll k_B T$, where the Ginzburg–Landau equations can be derived from the microscopic theory, it was shown that the very useful explicit expressions for ξ and λ in both the clean and dirty limits could be derived (such as, for example, the expressions given by Saint-James et al. [19]) and led to the identification $e^* = 2e$, $n_s = n/2$. The numerical coefficients are fixed with the convention that $m^* = m$, the free electron mass. Nevertheless, since the Ginzburg–Landau equations are limited to the range close to T_c , only properties that depend on the value of the order parameter and its phase can be handled.

It was found in the experiments that in very good atomically uniform crystals of superconductors, such as mercury [3] or indium [6] with a good Meissner state at low magnetic fields, $\mathbf{B} = 0$, upon application of a magnetic field, the domains appeared that were in the normal state (N) interleaved with domains that were in the superconducting state (S). The crystals studied had a mean free path for elastic scattering of the order of 0.5 mm, whereas the thicknesses of the N and S layers were inferred to be in the 0.02 mm range. In other words, the transport at the NS interfaces could definitely be considered ballistic.

In 1964, Andreev [1] used the Gorkov equations [11], applied to a system without impurity scattering, which contained a more or less sharp boundary between a normal phase and a superconducting phase. He found the conversion of an electron to a hole with a probability that depends on the energy relative to the energy gap Δ of the superconducting state. He proceeded by calculating the thermal flux across the boundary and compared the result with the data obtained by Zavaritskii. In passing, he pointed out that the path of the electron and the hole had a unique element to it: “*We note the following curious feature. Usually when particles are reflected, only the component of the velocity normal to the boundary changes sign. The projection of the velocity on the plane of the boundary remains unchanged. In our case all three components of the velocity change sign*”. It means that the reflection process is dependent on the energy, it inverts the charge, and it leads to a reversal of all velocity directions.

Although Andreev based his analysis on the Gorkov equations, the most common approach to discuss the process of Andreev reflection is now by using the Bogoliubov–De Gennes equations. However, Bogoliubov and De Gennes never wrote a paper together and it is therefore worthwhile to provide some indication on how these names came together. The emergence of the Bogoliubov formulation of the theory of superconductivity together with the construction of the Gorkov the-

ory is described by Gorkov [20]. Around 1963, Pierre Gilles de Gennes applied a Bogoliubov transformation to a position-dependent eigenfunction. He defines

$$\psi(\mathbf{r} \uparrow) = \sum_n [\gamma_{n\uparrow} u_n(\mathbf{r}) - \gamma_{n\downarrow}^* v_n^*(\mathbf{r})], \quad (5)$$

which represents the annihilation operator for a position eigenfunction, with u and v also position-dependent eigenfunctions to be determined from the effective Hamiltonian, with $\Delta(\mathbf{r})$ to be found self-consistently from

$$\begin{aligned} \Delta(\mathbf{r}) &= V \langle \Psi(\mathbf{r} \uparrow) \Psi(\mathbf{r} \downarrow) \rangle = \\ &= V \sum_n v_n^*(\mathbf{r}) u_n(\mathbf{r}) [1 - 2f_n]. \end{aligned} \quad (6)$$

From this starting point, De Gennes derived the set of coupled equations, which are now called Bogoliubov–De Gennes equations. They appeared for the first time in print in 1963 in [21]. It is stated that for a normal metal film on a superconductor, the one-particle excitation energies are the eigenvalues of

$$\begin{aligned} Eu &= \left(-\frac{\hbar^2}{2m} \nabla^2 - E_F \right) u + \Delta v, \\ Ev &= \left(\frac{\hbar^2}{2m} \nabla^2 + E_F \right) v + \Delta u. \end{aligned} \quad (7)$$

The “pair potential” Δ is defined as

$$\Delta(\mathbf{r}) = g(\mathbf{r}) \langle \psi(\mathbf{r}) \psi(\mathbf{r}) \rangle, \quad (8)$$

where $g(\mathbf{r})$ is the local value of the electron–electron coupling constant and the $\psi(\mathbf{r})$ is the usual one-electron operators.

This set of equations (Eqs. (7)), which obviously look like a set of Schrödinger equations coupled by the parameter Δ , are called the Bogoliubov–De Gennes equations. To the best of our knowledge, the assignment of these equations to these two authors together, and not for example to De Gennes and Saint James, was for the first time done in print in a paper by Kulik [22] on the supercurrent in an SNS junction. Historically, it is clear that the origin can be found in the self-consistent field method for the BCS theory of Bogoliubov [23], which was originally published in JETP [24] and Il Nuovo Cimento [25]. Kulik refers to another paper of Bogoliubov [26], which deals with general aspects of the self-consistent field method.

The actual derivation of the Bogoliubov–De Gennes equations is given by Saint-James in Ref. [27] in an appendix, while referring to lecture notes on the subject by De Gennes, dated 1963–1964, which were later published by De Gennes [28] in 1966. Ironically, in a

1964 paper on the excitations in a vortex core, Caroli, De Gennes, and Matricon [29] refer to the set of equations by simply citing Bogoliubov et al. [24]. Unfortunately, this hides a major accomplishment by De Gennes, which is the generalization of the Bogoliubov (u, v) transformation to the case of inhomogeneous systems. Shirkov [30], a former collaborator of Bogoliubov [24], calls it the Bogoliubov–De Gennes transformation (Eq. (5)) that can be written in terms of coordinate-dependent $u(\mathbf{r}), v(\mathbf{r})$ wave functions of electrons in the superconducting phase. The conclusion is that the major step forward by De Gennes was the generalization of the Bogoliubov transformation to position-dependent wave functions for the quasiparticles, through which he opened the door to treating ballistic inhomogeneous problems in superconductivity. It is therefore historically understandable to call the set of equations (7) the Bogoliubov–De Gennes equations. At the same time, it is clear that the Gorkov equations are more general and can be used as a starting point for also treating the cases with diffusive scattering and nonequilibrium problems.

Meanwhile, in the course of history, the significance of the contribution of Saint-James might have become underexposed. Interestingly, in the 1964 paper by Saint-James, we already find a glimpse of the phenomenon that we now call Andreev reflection. He published a more extensive calculation of the 1963 paper with De Gennes [21], using the Bogoliubov–De Gennes equations, for a normal metal of thickness a on a superconductor with the interface located at $x = 0$ to determine the excitation spectrum. At the end of this calculation, he writes in the French Journal de Physique: “*What is the origin of the result? An electron travels through the region (N), and penetrates in (S), where it creates an electron-hole pair. The two electrons combine to form a Cooper-pair, leading to a hole which travels back inside (N), after which it reflects at the opposite surface of (N) at $x = -a$ and the cycle will repeat. The total duration of the cycle is $4a/v_F \cos \theta^{r1}$* ”, with θ a measure of the energy. The factor 4 indicates that the slab needs to be traversed two times to provide interference, to be contrasted with 2 for normal reflection. Based on this article, Deutscher [31] has re-

¹⁾ Quelle est l’origine physique de ce résultat? Un électron s’avance dans la région (N), pénètre dans (S) où il crée une paire électron-trou. Les deux électrons se combinent pour former une paire de Cooper, tandis que le trou repasse dans (N), se réfléchit sur la surface $x = -a$ et revient dans (S) où il détruit une paire de Cooper. Un électron apparaît de nouveau, repasse dans (N), se réfléchit sur la surface et le cycle recommence. La durée totale de ce cycle est: $4a/v_F \cos \theta$.

cently argued that the phenomenon of Andreev reflection should be called Andreev–Saint-James reflection to do justice to the historical record. In our view, the unique nature of the process of Andreev reflection is the reversal of all velocity components, the unfamiliar process called retro-reflection, which is fully recognized and understood for the first time in the original Andreev paper [1]. Therefore, we believe it is justified to continue to speak about the concept of Andreev reflection, meaning the reversal of all velocity components and the charge.

The framework of the Bogoliubov–De Gennes equations (Eqs. (7) and (8)) allows describing a nonuniform superconducting state in many selected cases of current interest. The parameter V in Eq. (6) is responsible for the attractive interaction leading to superconductivity. The quantity Δ can be present anywhere, expressing what is called the proximity effect. The Bogoliubov–De Gennes equations have been used extensively to determine the excitation spectrum for materials in which the normal and superconducting phase coexist under certain conditions. Examples are the excitations in the core of a vortex [21], the excitations in the normal domain of a type-I superconductor in the normal state [32], and the excitations in an SNS type Josephson junction by Kulik [22]. In the last two cases, the calculation is usually carried out for a one-dimensional model.

Most experiments were carried out on high-purity, well-annealed single crystals of tin, indium, mercury, or lead. In these samples, the elastic mean free path easily reaches a size approaching a millimeter. Therefore, it was natural to ignore elastic scattering and to treat the wave functions as plane waves. A direct measurement of the excitation spectrum had to wait, in all three cases, until the arrival of nanolithography and scanning probe techniques. On the other hand, the concept of Andreev reflection nicely explained the observed difference between the electrical and thermal conduction at NS interfaces. The remaining question is what direct experimental evidence has been accumulated to test the theoretical ideas in a qualitative and quantitative way. How would we experimentally access a well-defined normal-metal–superconductor interface, for which we can qualitatively and quantitatively study the process of Andreev reflection itself?

4. BALLISTIC TRANSPORT AND ELECTRON FOCUSING: 1966, 1974

In hindsight, in order to be able to study and exploit the phenomenon of Andreev reflection in its full

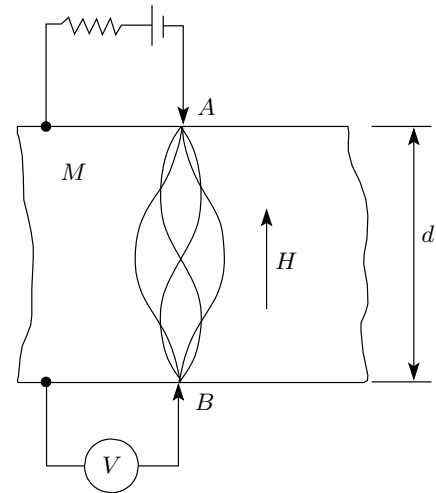


Fig. 2. Ballistic trajectories in a pure crystal following paths controlled by the Fermi surface. Point contact A acts as the emitter and point contact B as the collector. A magnetic field is applied in the direction of the electron flow. (Picture taken from Sharvin and Fisher [33])

potential, we need a source of quasiparticles, a collector, and a medium through which their properties are manifest. One of the first steps along this path was set by Sharvin [13], who introduced a new technique to study Fermi surfaces by putting a sharp metallic needle on a bulk single crystal of a metal as a source and a second one at the opposite side as a collector (Fig. 2). The electrons would follow paths along the Fermi surface and the trajectory between the source and the collector could be influenced by a magnetic field. In his analysis, he treated the point contact as ballistic, i. e., with a size small compared to the elastic mean free path in the material of the needle as well as of the crystal. From this assumption, he inferred that the current is the difference between electrons coming from one reservoir at a voltage V , while the other reservoir, kept at ground, sends electrons in the other direction. The “Sharvin” resistance is then given by

$$R = \frac{p}{e^2 D^2 N}, \quad (9)$$

where D is the diameter of the hole forming the point contact, p is the Fermi momentum, and N is the electron density. A first observation was carried out by Sharvin and Fisher [33] and in more detail, by Sharvin and Bogatina [34]. Since the mean free path is much larger than the diameter of the orifice D , the resistance is not the familiar backscattering resistance inside the

constriction, but rather the geometrical restriction on possible conduction channels.

This pioneering work with point contacts to understand fundamental transport processes led to two new types of experiment. Yanson [35] recognized in 1974 that the concept of ballistic transport through an orifice as introduced by Sharvin was useful to understand “failed” tunnel junctions. Applying a large voltage to a tunnel barrier produces one or more leaky pathways, which can be analyzed as a Sharvin contact. He went one step further and pointed out that the current–voltage characteristic might contain nonlinearities due to a backscattering current resulting from phonon excitation, which should reveal the electron–phonon interaction spectrum. It was known that the latter was measurable with superconducting tunnel junctions. This new point-contact technique allowed measuring the electron–phonon interaction in normal metals. The success was demonstrated for copper by Yanson and Shalov [36]. It inspired a group in Nijmegen in the Netherlands, led by Peter Wyder (who had interest in point contacts for far-infrared detection; see next section) to apply the same reasoning to the point contacts as used by Sharvin. First results of this technique applied to copper, silver, and gold were published by Jansen et al. [37] and the method was popularized by a publication in *Science* by the same authors [38].

A second development was introduced also in 1974 by Tsoi [39, 40]. He modified the technique of Sharvin to follow the paths of the electrons by putting the source and the collector on the same side of the crystal. By using a transverse magnetic field, he was able to tune the cyclotron orbits in such a way that for certain specific strengths of the magnetic field, the emitted electrons would reach the collector preferentially, also reflecting the Fermi-surface properties. This technique was also adopted by the Nijmegen group, leading to a collaboration between the groups at Chernogolovka and at Nijmegen [41].

This work with point contacts has laid the groundwork for an understanding of transport in terms of classical ballistic trajectories. It meant a concept of electronic transport in which two equilibrium reservoirs are connected through a small orifice with a radius a , which has the net resistance

$$R = \frac{4\rho l}{3\pi a^2} \quad (10)$$

with ρl , the so-called ρl -product, given by the free-electron values: mv_F/ne^2 . Electrons passing through the orifice are absorbed by the reservoir, where they equilibrate, and conversely, the reservoirs act as sources of equilibrium electrons.

5. JOSEPHSON POINT CONTACTS: 1966, 1979

In parallel to the research on the use of normal metal point contacts, there was quite a bit of research of a more applied nature on superconducting point contacts such as the one shown in Fig. 1. Superconducting point contacts have been extensively used in early developments of SQUID magnetometers and in demonstrating the response to radiation known as Shapiro steps. Undoubtedly, one of the beautiful aspects of the Josephson effect is that it is a macroscopic quantum phenomenon, which can occur in any kind of weak links, between two superconductors. Whatever the type of the weak link, if the coupling is not too weak to be disrupted by thermal or quantum noise, any material put between the two superconductors, even vacuum, would offer a manifestation of the basic characteristics of the Josephson effect. After the initial observation in a tunnel junction by Rowell and Anderson, it was quickly followed by a demonstration of the ac Josephson effect in a superconducting microbridge, sometimes called an Anderson–Dayem [42] bridge. In 1966, Zimmerman and Silver [43] introduced a DC SQUID based on two mechanically-made point-contact diodes, very much like the Sharvin point contacts. The technique of using point contacts was quickly taken up by researchers interested in an excellent coupling to microwave radiation. Dayem and Grimes [44] studied the emitted radiation of a point contact biased at a certain voltage. Levinstein and Kunzler [45] showed that a point contact made it possible to obtain current–voltage characteristics which evolve from a tunneling curve to a typical point contact IV curve, whose nature was not yet fully understood at that time. Grimes, Richards, and Shapiro [46, 47] turned the point contact into a detector of far-infrared radiation. The technical details of their apparatus have been described by Conaldo [48].

Meanwhile, the scientific concepts around the point contacts of Zimmerman and Silver were quite different from those of Sharvin. For Zimmerman and Silver, the microscopy of the Sharvin point contact appeared to be completely absent. The emphasis was on the electromagnetic performance. Since all of the point contacts, as well as the microbridges, had a low normal state impedance, it was understood by Stewart [49] and McCumber [50] that the most appropriate engineering model was that of the resistively shunted model (RSJ model), which could be shunted by a capacitor and is therefore often called the RSJC model. This RSJC model treated the point contact as a Josephson element characterized by the celebrated Josephson equa-

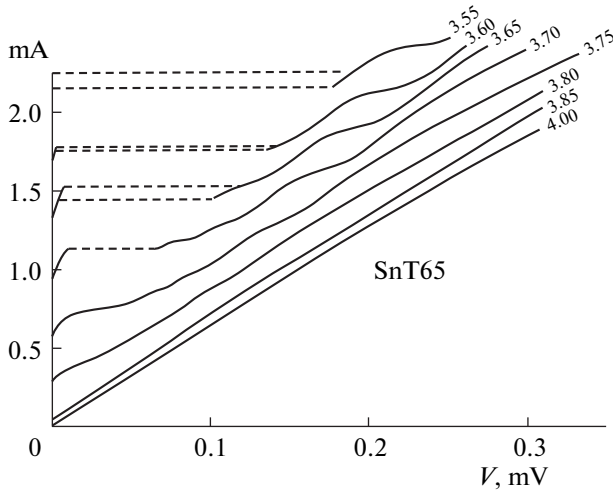


Fig. 3. Typical current–voltage characteristics for variable-thickness microbridges, made of superconducting tin. These curves clearly show all the salient deviations from the RSJ model: a resistive state at low voltages with a slope much smaller than the normal state resistance, a subharmonic gap structure, and an excess current. The data are all taken close to T_c because at lower temperatures, thermal hysteresis dominates and masks the interesting physics. From Klapwijk et al. [51]. The numbers at the curves indicate the bath temperature

tions and shunted by a capacitor. This model made it possible to understand the dominant difference between a Josephson tunnel junction and a low-capacitance current-biased point contact or microbridge. It also made it possible to identify at which level of capacitance hysteresis would appear in the IV curve. The Stewart–McCumber model became the paradigm for all research in which a microscopic understanding was not needed or not sought. In reality, there were very many deviations (see, e. g., Figs. 3 and 4), which were temporarily ignored. It is still the dominant model for experiments in which the Josephson junction functions as a building block for macroscopic quantum tunneling.

In the former Soviet Union, research on point contacts and microbridges aimed at the interaction with high-frequency radiation was picked up at several laboratories of the Academy of Sciences. Early work was found at the Institute of Physics Problems by Khaikin and Krasnopolin [53] in 1966. A strong program led by Vystavkin and Gubankov emerged at the Institute of Radioengineering and Radioelectronics of the Academy of Sciences around 1970. Working at this laboratory Volkov and Nad’ [54] published experimental data and a theoretical analysis of Shapiro steps

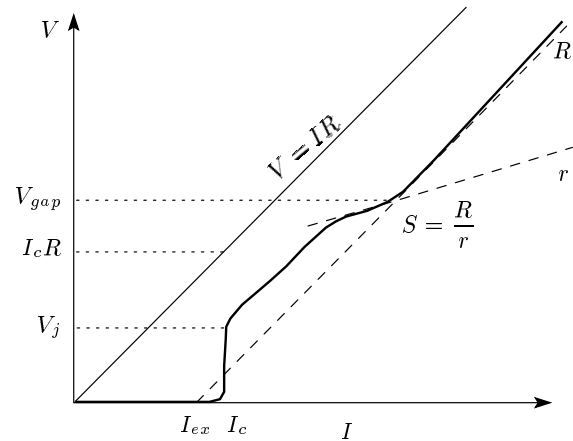


Fig. 4. Current–voltage characteristic for a ballistic niobium point contact with ideal equilibrium reservoirs (taken from Weitz et al. [52]). It clearly shows the excess current beyond V_{gap} as well as the overall deviations from the resistively shunted junction model. Similar IV curves have been obtained for niobium tunnel junctions with a “leaky” silicon barrier

observed in niobium point contacts, using the theory presented by Aslamazov and Larkin [18], which in essence is the Stewart–McCumber model. The interest in constriction-type Josephson junctions is clear from the 1974 review paper by Vystavkin et al. [55], in which research at the IREE is presented together with work by Likharev at Moscow State University. Both point contacts and superconducting microbridges were developed and studied. The majority of the work was focused on the Josephson effect and interpreted in the framework of the RSJC model. However, as in many other groups, significant deviations from the RSJC model were observed. In a number of cases, the solution was sought within the lumped circuit nature of the RSJC model. Although there was a strong drive towards using Josephson junctions for practical applications, a number of people stepped out of that mode and focused on an improved microscopic understanding. In reality, a new microscopic theoretical framework, largely absent in the well-known 1979 review by Likharev [17], was needed to deal with inhomogeneous problems in nonequilibrium superconductivity.

6. DIFFUSIVE NONEQUILIBRIUM THEORY: 1968–1979

The Bogoliubov–De Gennes equations had emerged as suitable in dealing with inhomogeneous problems in systems with little or no impurity scattering. How-

ever, the superconducting devices that were of interest for practical applications, the point contacts and microbridges, were made of materials that had significant impurity scattering. The nature of the contact of the point contact was not very well known, but given the crude way of making them, elastic scattering inside the contact was to be expected. Microbridges were made from vacuum-condensed thin films and made with diamond-knife technology or primitive lithography. To describe these inhomogeneous superconducting systems, including impurity scattering, an appropriate theoretical framework was urgently needed.

In the late 1960s and early 1970s, the quasiclassical theory for inhomogeneous and nonequilibrium superconductivity was developed. It started with the Gorkov theory [11], with the subsequent developments primarily in the former USSR with significant contributions in Germany. A general introduction is available in the textbook by Kopnin [56]. An overview convenient in the context of mesoscopic systems is provided by Belzig et al. [57]. For the topic addressed here, the main message is that this framework provides a microscopic theory for inhomogeneous systems, which is valid for all temperatures and which is also suitable for nonequilibrium systems. Therefore, the theory is particularly well suited, although not always easily tractable, for superconducting constrictions such as microbridges and point contacts, including cases where the scattering is diffusive. The theory is, in principle, also well-suited to deal with the large variety of modern hybrid devices in which nano-objects are coupled to superconducting electrodes.

The starting point is the field-theoretical description of superconductivity introduced by Gorkov [11], which has evolved into the quasiclassical theory by removing the rapid oscillations on the scale of the Fermi wavelength by Eilenberger [58] and Larkin and Ovchinnikov [59]. To deal with finite temperatures, the Matsubara [60] frequencies and Keldysh [61] techniques are used. A distinction can be made between clean and dirty systems, resulting for dirty systems in the theory for nonequilibrium inhomogeneous superconductivity problem of Schmid and Schön [62] and Larkin and Ovchinnikov [63, 64].

The approximations made over this 10-year period have been very helpful in making the theory usable for the study of Josephson devices such as point contacts and microbridges. It was applied to a number of outstanding problems in the field of superconducting contacts. In contrast to tunnel junctions of which the quasiparticle current branch, the Giaever tunneling was understood even prior to the discovery

of the Josephson effect, the voltage-carrying state of superconducting point contacts contained a number of poorly understood phenomena (see, e. g., Fig. 3). First, when exceeding the critical current, a steep increase in the current, at finite voltage, is observed up to a few microvolts, after which the voltage increases much more rapidly and often discontinuously. This “knee-structure” or “foot-structure”, depending on whether the voltage or the current is plotted horizontally, was observed in various laboratories and violated the elementary RSJ model. In addition, upon a further increase in the current, the well-known subharmonic gap structure, features in the IV curve at $2\Delta/n$ are observed, followed by a so-called excess current beyond 2Δ , a shifted asymptote suggesting a capacity to carry more current at the same voltage than in the normal state. A very clear example of the excess current can be found in Weitz et al. [52] and reproduced in Fig. 4. These phenomena were universally observed in all constriction-type superconducting contacts, such as the microbridges, “pinholes” in tunnel junction barriers and in point contacts. To cover a sufficiently large range of temperatures and voltages, an important requirements was the use of large reservoirs to maintain thermal equilibrium in the contacts, which for microbridges led to the use of variable-thickness bridges.

The first item, the “knee-structure”, was addressed by Golub [65] and Aslamazov and Larkin [66], followed by an improved analysis by Artemenko, Volkov, and Zaitsev [67, 68] and in a more accessible way by Schmid, Schön, and Tinkham [69]. The essential interpretation is that under the voltage bias, the density of states in the neck of the constriction oscillates rapidly at the Josephson frequency. The current carried by this rapidly changing density of states behaves differently for energies $E < \Delta$ and $E > \Delta$. The first part can, upon changing in time, only be populated by quasiparticle relaxation caused by inelastic processes. The second part can easily equilibrate by diffusion to the equilibrium banks. The models assume a short one-dimensional diffusive superconducting wire connected to massive equilibrium reservoirs of the same superconducting material.

The third item that was addressed was the “excess current”. Artemenko et al. [68, 70] showed in 1978–1979 that this excess current was not related to the Josephson effect, in other words, unrelated to the physics contained in the RSJC model, but was part of the static quasiparticle current through the constriction. A quite striking breakthrough came by a comparison of experimental results between S–c–S contacts and S–c–N contacts in research reported by Gubankov et al. [71]. It

led to the decisive article of Artemenko et al. [72], in which the theoretical results for the excess current in both S–c–S and S–c–N contacts were presented. In that paper, the authors write: “*Therefore, particles with energies $|E| < \Delta$ contribute to the current in the bridge. Naturally, the gap in the S-region does not prevent the charge transfer by the electrons with the energy $|E| < \Delta$. The current transferred by these particles converts into the pair current in the S-region. Note that the analogous process (called the Andreev’s reflection) takes place in a pure metal when electrons pass through the ideal S–N interface*”. The message that the much more transparent concept of Andreev reflection was hidden underneath the heavy mathematical formalism was brought by Michael Tinkham to his PhD students and one of his post-docs (one of the present authors) from a visit to Moscow in 1978. Without this explicitly made connection with the concept of Andreev reflection, it would have been much more difficult to appreciate the major step forward in understanding constriction-type superconducting devices. It proved that a microscopic analysis was needed to understand the voltage-carrying state not only of tunnel junctions but also of point-contact devices and that the RSJ model was misleadingly lacking relevant microscopic input. With the word Andreev reflection for the IV curves of Josephson point contacts on the table, the conceptual framework for constriction-type Josephson junctions had to turn from phenomenological to microscopic. (The concept of Andreev reflection already appeared in the work of Artemenko and Volkov [73] for the electrical resistance in the intermediate state based on the kinetic equations for clean superconductors proposed by Aronov and Gurevich [74]. So they were conceptually very well prepared.)

7. DIRECTION, CHARGE, AND ENERGY DEPENDENCE OF BALLISTIC ANDREEV REFLECTION: 1980–1984

The theory of Artemenko et al. was based on diffusive superconductors in which the elastic mean free path is much shorter than the BCS coherence length and also than the size of the constriction. The concept of Andreev reflection was much more tailored to the picture of plane waves emanating from reservoirs analogous to the ideas of the Sharvin point contact and the subsequent implementation by Yanson and Jansen et al. for electron–phonon spectroscopy and by Tsoi et al. for electron focusing. After the insightful remarks about the relevance of Andreev reflection, the

natural starting point to take for a point contact and for microbridges was the idea of a ballistic point contact, analogous to the flow resistance of an orifice in the Knudsen gas limit. It sets the starting point for an interpretation of the second item mentioned in the preceding section of the subharmonic gap structure by Klapwijk, Blonder, and Tinkham [75]. By allowing for energy-conserving multiple Andreev processes, it became immediately plausible that the subharmonic gap structure had to be understood in the same framework as the excess current, and that it was a different form of the quasiparticle current flow, analogous to Giaever tunneling but now including higher-order processes. (This was quite different from the starting point for the Josephson current known from the ballistic model of Kulik [22] and Bardeen and Johnson [76], because the process was considered to be not due to the Josephson effect.) A description was found on the basis of the trajectory method and presented as an invited talk, resulting from rumors that we had something new to tell, at the Low Temperature conference in Los Angeles (18–23 August 1981) and published in the proceedings [75]. It contained the description of the IV curve of an NS point contacts subject to both Andreev reflection and normal reflection located at the neck of the constriction:

$$I = \frac{1}{eR_n} \times \int dE [1 + A(E) - B(E)] [f(E - eV) - f(E)]. \quad (11)$$

The function $A(E)$ is called the Andreev reflection coefficient. For $E < \Delta$, it should ideally be 1, reflecting perfect electron–hole conversion, which would unavoidably occur at a sharp interface between the superconducting phase and the normal phase in an atomically uniform material, such as in the intermediate state:

$$A(E < \Delta) = \frac{\Delta^2}{E^2 + (\Delta^2 - E^2)(1 + 2Z^2)^2}. \quad (12)$$

The function $B(E) = 1 - A(E)$ for $E < \Delta$ is the elastic backscattering, which would be present for any elastic-scattering process at the interface. It is parameterized by Z , which is connected to the normal-state transmission coefficient T by $T = 1/(1 + Z^2)$. For $Z = 0$, indeed, $A = 1$ and $B = 0$. A similar expression controls A and B for energies above the gap, $E > \Delta$. Of course, for high values of E , the Andreev reflection goes to zero, but up to about 3Δ , there is still a significant contribution. In relation to practical experiments, an important aspect is the sensitivity to Z or the normal state transmission coefficient. For $Z = 1$, which reflects

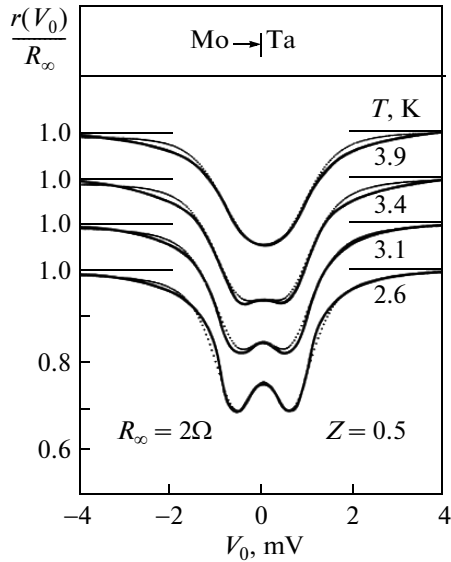


Fig. 5. One of the first point-contact experiments showing the energy-dependent Andreev reflection coefficient weighted by the distribution functions. The fits are for the same set of parameters, with only the temperature being varied. From Voss [82]

a transmission probability of 0.5 (one would normally call it a very high transmission), the Andreev reflection probability has declined for $E = 0$ by a factor of 10. This illustrates the high sensitivity to elastic scattering, which is important to superconducting hybrids. In Fig. 5, one of the first comparisons with these theoretical predictions is shown using a molybdenum–tantalum point contact. With Z as the only fitting parameter, all the other curves are generated using Eq. (11).

Since the trajectory method did not have a cut-off for higher orders, all contributions weighed equally and the subharmonic gap structure disappeared at lower temperatures. The obvious step to take was to introduce a finite transmissivity of the constriction, but the authors did not see a way to handle this. This led to an analysis of the much simpler problem of a ballistic S–c–N contact, which became the now well-known BTK paper [14]. In a subsequent analysis, we returned to the S–c–S case by putting two N–c–S contacts together [77], although we knew that this failed to describe the system properly, in particular, for low transmissivities of the double-barrier elastic potentials. While we were doing this work, we received a copy in Russian of an article published by Zaitsev [78], in which he treated the S–c–S and the S–c–N case in the ballistic limit. It made us a bit nervous about the originality of our work. On the other hand, he treated only a fully transmissive case,

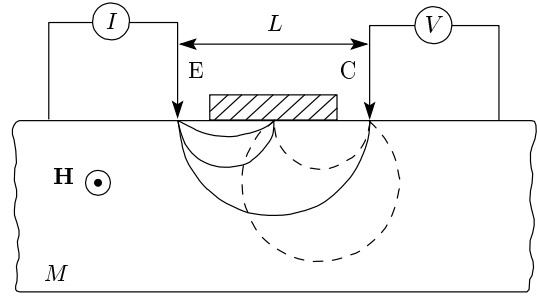


Fig. 6. A single crystal of bismuth is partially covered with a thin film of tin with a critical temperature of about 3.8 K. Electrons injected at point contact E reach collector C following classical trajectories controlled by the magnetic field \mathbf{H} . Full curves are electron trajectories, dashed curves are hole trajectories after Andreev reflection below T_c . Taken from [85]

without any elastic scattering, which we felt was our most important innovation. Moreover, he predicted an enhancement of the conduction by a factor of 3, which we saw as a sign that despite the mathematical skills, the physical content was not fully appreciated (an erratum appeared soon) [79]. Undoubtedly, the major step forward we made was the inclusion of elastic scattering, which became possible within the formalism that Zaitsev used, only after the introduction of new boundary conditions in 1984 [80].

One of the very interesting aspects of the BTK paper is that it made it possible by a simple point contact technique, pioneered by Sharvin and developed further by Yanson, Jansen et al., and Tsoi, to read off the energy dependence of the Andreev reflection coefficient, as already appearing in the original paper by Andreev in 1964, from the derivative of the IV curve. We emphasize the energy dependence, as was clearly shown by Blonder and Tinkham [81], but was in retrospect already present in the data of Gubankov et al. [71]. The first systematic use of this opportunity, shown in Fig. 5, in which a set of conductance curves is given for a Mo–Ta point contact from the PhD Thesis of Gerhard Voss [82] (a student of Wohlleben) in Cologne. The quantitative success and the detailed dependence on the energy led to the emergence of Andreev point contact spectroscopy. Another important aspect is the ballistic nature of the assumed conduction of the contact, which is apparently justified despite the crude fabrication technology. The simplicity of the technique has allowed using it in a laboratory course to train undergraduate students [83].

The ballistic Sharvin-type point contacts have al-

lowed directly measuring the energy dependence of the Andreev reflection coefficient, which has now been applied to a large variety of superconducting materials and the relevant theory has been generalized. Very recently, the Sharvin point-contact idea was also extended to apply to correlated materials by Lee et al. [84]. Nevertheless, one of the hall-marks of Andreev reflection is the idea of retroreflection. This is universally assumed to be one of the properties contained in the experimental data and sometimes explicitly assumed in the calculations. However, a direct demonstration of retroreflection itself is an interesting experimental challenge. The explicit demonstration started in the work Sharvin and Tsoi on point contacts with high-purity crystals. A direct demonstration was carried out by Bozhko et al. [85] at Chernogolovka and Benistant et al. [86] in Nijmegen using what is called electron focusing. It requires the ballistic transport from a point contact used as an emitter, the reflection from a superconductor, and the subsequent absorption by a second point contact that serves as a collector (Fig. 6). Depending on the strength of the magnetic field, the cyclotron orbits coalesce at the absorbing point contacts. At specific values of the magnetic field, the lowest value given by $B_{focus} = 2\hbar k_F/2L$ with L being the distance between the emitter and the collector, a maximum signal is found. With increasing the magnetic field, two peaks are found. For elastic scattering, these are two with the same sign. For Andreev reflection, a second one has an opposite sign because of the opposite charge. And if it is indeed retroreflection, the hole trajectories should be copies of the electron trajectories. This is exactly what is found and shown in Fig. 7. This last point-contact experiment completed the demonstration of the essential ingredients of Andreev reflection: the energy dependence, the charge reversal, and time-reversed paths.

8. QUANTUM TRANSPORT IN A POINT CONTACT: 1988

In the 1980s, the world of mechanically-made point contacts was gradually being transformed into a world of nanostructures made through clean-room technology. In this transition, the concept of Andreev reflection became fully embedded in the nanoworld. However, the first step was to take the idea of a Sharvin point contact from a classical concept with ballistic trajectories into the currently dominant paradigm of quantum transport. In the normal state, the transport properties in small-scale structures are treated with the

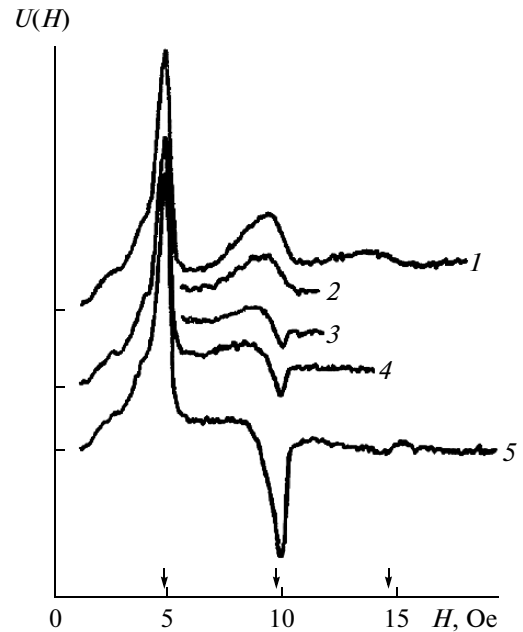


Fig. 7. The electron-focusing signal observed in the collector contact for temperatures 3.80, 3.78, 3.74, 3.70, and 2.78 K from top down. It clearly shows the emergence, at a field strength of 10 Oersted, of an initially positive contribution, which becomes negative for lower temperatures. A very clear proof of the (almost) identical but reverse, momenta and of the charge reversal. Taken from [85]

transmission-matrix formalism. Since the devices became small enough such that quantum coherence was maintained over the size of the device, transport became dominated by quantum interference. The emergence of this approach has greatly benefited from the increasing capability of making metallic structures on a nanoscale with lithography, in particular, electron-beam lithography. Research objects from condensed-matter systems were made in which the length scale became a very important parameter. The research objects are often called nano-devices or nano-structures, although in particular the name “device” is somewhat misleading. They are usually not intended to provide real functionality, but rather to serve as a vehicle to reveal physical phenomena. In that sense, it is part of the experimentalist’s toolbox. For some, the Large Hadron Collider in Geneva is the experimental system to do scattering experiments with, for others, it is a nano-device of which many can be made in clean rooms worldwide. In combination with a superconductor, a nanodevice is unavoidably an inhomogeneous superconducting system. It consists of different assemblies of

atoms in which different states of matter can occur. The central concept to describe their transport is the scattering matrix, consisting of asymptotically-free incoming states through an interaction region and providing free outgoing states. A recent review on the theoretical aspects is provided by Lesovik and Sadovskyy [87]. It is particularly specific about the way in which it is justified in comparison to the more conventional kinetic equation and Green's function approaches and also as regards the assumptions that are made and have to be satisfied in experimental systems.

The resistance in the normal state in the BTK result was clearly in the spirit of the early proposition of Landauer [88] about electrical conduction as a quantum transport phenomenon and is given by

$$G = \frac{e^2}{\pi\hbar} \frac{T}{R}, \quad (13)$$

where G is the conductance of a conductor and T and R are the transmission and reflection coefficients. The Landauer formula, Eq. (13), has been generalized to multi-channels by Büttiker et al. [16] and is expressed as

$$G = \frac{e^2}{\pi\hbar} \sum_{n,m=1}^{N_c} |t_{nm}|^2, \quad (14)$$

where t_{nm} is the transmission coefficient for scattering through the contact from incoming channel n into outgoing channel m . The case with no elastic scattering in the wire, the perfect Sharvin contact, corresponds to $|t_{nm}|^2 = \delta_{nm}$. This appealing scattering-matrix approach was introduced to deal with normal transport in small structures with a length smaller than the phase-breaking length, over which phase coherence was preserved.

At about the same time, the discovery of the quantum Hall effect in 1980 by Von Klitzing et al. [89] in silicon MOSFETs, followed by the discovery of the fractional quantum Hall effect by Tsui et al. [90] in GaAs/AlGaAs heterostructures, led to a strongly increased interest in 2-dimensional systems with a high mobility. Prior to the discovery of these systems, the ballistic transport could be realized only in large single crystals of well-behaving metals. With the semiconductor technology, new artificially-made systems became available and were continuously improved. These semiconductor heterostructures provided a 2-dimensional analogue of the large single crystals of the past with the advantage of being a fully 2-dimensional systems where the carrier density could also be changed with a gate.

These two developments, the microfabrication tools and the availability of new forms of matter in the form

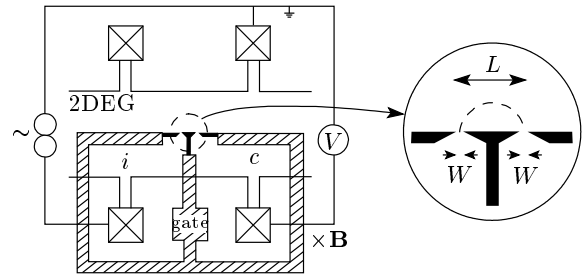


Fig. 8. The experimental arrangement of the gates on top of a GaAs/AlGaAs 2-dimensional electron gas (2DEG). By changing the gate voltage, the 2DEG is depleted and transport is only possible in the gaps forming the point contacts. Given the low carrier density of the 2DEG compared to a metal, the transport was found to be quantized. The design was made to allow for an electron-focusing experiment analogous to the one carried out by Tsoi et al. [39]. Figure taken from [93]

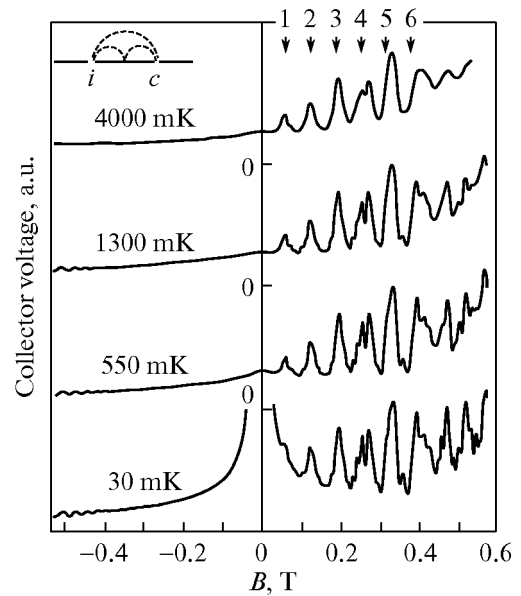


Fig. 9. The electron-focusing signal observed in the collector contact for a range of temperatures, clearly illustrating the ballistic nature of the transport. Because of the phase coherence, fluctuations were observed reflecting the fact that the description has to go beyond the classical trajectories (and of course evolves into the quantum Hall effect). Figure taken from [93]

of heterostructures, came together in experiments carried out in a collaboration between Philips Research Laboratories and Delft University of Technology. Inspired by the point contact electron focusing experiments carried out by Tsoi et al. [39] and by Van Son

et al. [91] on single crystals of metals like silver, a two-point contact geometry was designed for a 2-dimensional electron gas in GaAs/AlGaAs (Fig. 8). The transport through one of these point contacts led to the surprising, but rapidly understood, discovery of quantized transport by Van Wees et al. [92]; the paper was submitted on Dec. 31, 1987. The electron-focusing experiments, exploiting the two contacts together (Fig. 9), were published separately by Van Houten et al. [93] and submitted one week after the quantum point-contact paper, on Jan. 6, 1988. This particular development towards the discovery of quantum transport, simultaneously with Wharam et al. [94], inspired by a different conceptual tradition, shows nicely how the original idea of Sharvin on point contacts and of Tsoi on electron focusing had found its way to the modern lithography applied to condensed-matter structures, based on semiconducting heterostructures. Apparently, unaware of these recent developments, Tsoi et al. in a review in 1989 [95] expected a development to use electron focusing in the study of Andreev reflection in lithographically-made structures.

9. MECHANICAL BREAK-JUNCTIONS: SUPERCONDUCTING QUANTUM POINT CONTACTS: 1992

The description of quantum transport with the transmission-matrix formalism has clearly a strong appeal also for superconductivity. It can easily be integrated with an analysis based on the Bogoliubov–De Gennes equations, assuming a ballistic transport system. An important problem is that a number of assumptions are made, which are often difficult to meet in an experiment. As summarized clearly in Büttiker et al. [16], the model system consists of three ingredients. There is a “sample”, which is characterized by a transmission matrix with the elements t_{nm} . There is no energy relaxation in the sample and transport through the sample is phase coherent. The sample is connected on both sides to “leads”, which only serve to transport plane waves back and forth with probability 1. Hence, they do not contribute to the scattering process. The leads are connected to “reservoirs”, which serve as equilibrium baths of electrons with a certain chemical potential and temperature. The value can be different in both reservoirs to represent an applied voltage difference.

These assumptions are very reasonable for the conventional metallic point contacts. They are also valid for the quantum point contacts in a 2-dimensional elec-

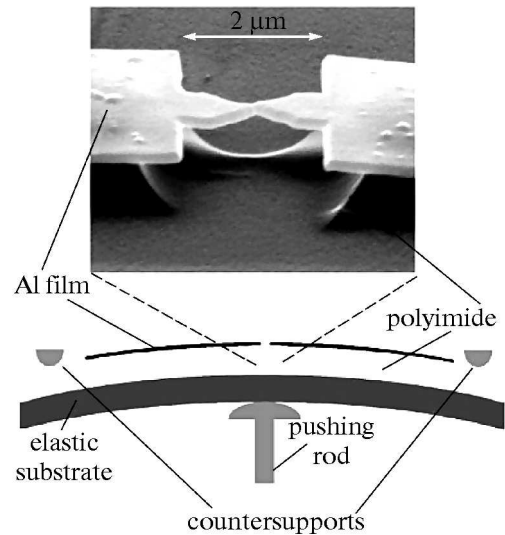


Fig. 10. A junction with a controllable break. Such a configuration allows gently breaking a wire, after which the two clean pieces can be brought together to form a vacuum tunnel contact, which evolves into a single-atom point contact. Figure taken from [97]

tron gas, described in the preceding section. With the split-gate technique, the major part of the 2-dimensional electron gas is unaffected. Only at some point, a constriction is created whose width can be adjusted. The reservoirs are therefore of the same material as the constriction. The real physical contacts to the apparatus do not play a role, because the wide sections of the 2-dimensional electron gas serve as the equilibrium reservoirs. The system is fully homogeneous in its properties, only the geometry of the conduction channel is changed.

Achieving similar experimental conditions for a quantum transport channel with a superconductor is much harder. The unavoidable solution is to combine two different materials, one that provides superconducting reservoirs and the other that acts as the “sample”. These systems are therefore called “superconducting hybrids”; we return to them below.

The most natural link with the assumptions of the transmission matrix for superconducting nanotransport is that of the mechanical-break junctions [96] with an example shown in Fig. 10. By breaking a wire, which can then be gradually brought together again, single-atom point contacts are created. The quantum conductor and the reservoirs are made of the same material in analogy to the GaAs/AlGaAs point contacts. In Fig. 11, the left panel shows a set of IV curves for single-atom contacts of aluminium [97, 98]. From bot-

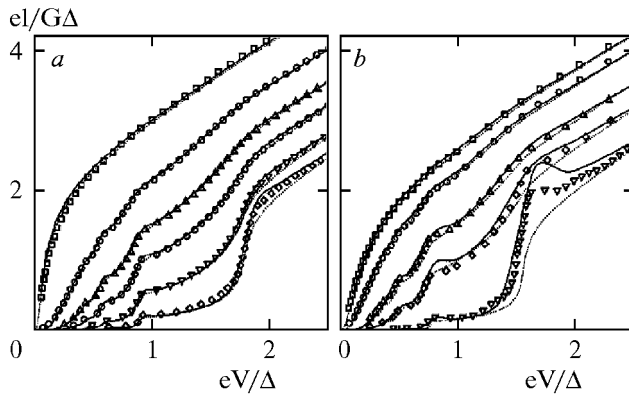


Fig. 11. A set of IV curves for increasing contact strength for Al (panel *a*) and for Au, which is part of a bilayer of Al on top of Au (panel *b*). Note the excellent agreement between theory and experiment in panel *a*. In panel *b*, a clear demonstration is given of how multiple Andreev reflection is created by an induced pair correlation in Au, with some minor deviations accounted for by the theory. Figure taken from [98]

tom up it shows the evolution of the IV curve from weak contact to stronger contact. It is a modern version of the old Sharvin point contact with the clean-room technology used to make a device that allows the breaking of a wire and the readjustment to bring the broken pieces together with subatomic precision. The data contain the same features observed in earlier generations of constriction-type Josephson junctions. They include the phenomenon of multiple Andreev reflections or multiparticle tunneling, leading to structure at voltages of $2\Delta/n$ and an excess current beyond a voltage of 2Δ . In Fig. 11*b*, a similar set of curves is shown for a single-atom Au contact. However, the Au is part of a bilayer with Al. The Au has become superconducting through the proximity effect. The experiment very nicely illustrates how the Andreev reflections are coupled to the induced superconducting order in Au. The differences can be largely accounted for by the standard diffusive proximity-effect theory using the quasiclassical equations.

Since the tunneling strength is tunable by the delicate adjustment between the atoms, both sets of curves can be understood as being due to a limited number of conduction channels, related to the orbitals of the aluminium or gold atoms. With increasing the coupling strength, the transmission coefficients get closer to unity, and the visibility of the structure weakens because higher-order processes are less damped. And because the material is the same, there is no left-over

mismatch between the two contacts limiting the transmission coefficients except for the orientation of the orbitals. This superconducting experimental system has the strong advantage that all experimental components of the quantum transport problem consist of the same material.

10. SUPERCONDUCTING HETEROHYBRIDS: 1985, 1990–1992

The interest in superconductors in combination with semiconductors was initially not just driven by interest in quantum transport. It was also in response to the collapse of the superconducting Josephson-computer program. From the mid-1960s, the Josephson tunnel junctions had received widespread attention because of the program at IBM, Bell Labs, NIST, and various Japanese and European Laboratories to develop a digital Josephson computer, which would be fast and have a low power consumption. Around 1983, this highly visible Josephson-computer program of IBM was cancelled (earlier already at Bell Labs, and elsewhere it was quickly considerably reduced). In the aftermath, it was extensively discussed that a Josephson junction had an important drawback. It is a 2-terminal device, unlike the very successful semiconductor transistor, which is a 3-terminal device with gain: the output voltage, for example, can be larger than the input voltage. The gatability of a semiconductor as part of a superconducting device or some other scenario might help.

Meanwhile, many university laboratories with interest in superconducting thin films started to use lithography and advanced electron-beam lithography with modified SEMs. The interest in small-area Josephson tunnel junctions led at Bell Labs in 1977 to the very research-friendly Dolan–Dunkleberger [99, 100] stencil lift-off technique, often called shadow evaporation. Initially introduced as a technique for advanced photolithography, it was, with the advent of electron-beam lithography, quickly used in the dimension range of hundreds of nanometers. It allowed the development of thin-film devices consisting of multiple materials overlapping in certain areas with or without an oxide barrier in between. Therefore, it was possible to combine superconductors with a normal metal, connected in multiple ways, and, for example, to measure the local density of states using Giaever tunneling. The same technique of shadow evaporation was also used to study phase-coherent normal transport on a short-length scale, related to the subject of weak localization,

which arose at the end of the 1970s, with the scaling theory of localization in 1979 as the famous hallmark. On the fundamental side, the discovery of the quantum Hall effect in 1980 and of quantized conductance transport in 1988 led to the increased interest in high-mobility semiconductor heterostructures, in particular, if this could be combined with superconducting contacts.

Although all these structures may be on a nanoscale, we call them “superconducting heterohybrids” in this section because we are particularly interested in the path to ballistic transport, which appeared to be available in high-mobility heterostructures. The goal is to combine semiconductor heterostructures with superconducting contacts following a top-down technological path. Another kind of superconducting hybrids is based on independently-made nano-objects, through a bottom-up process, which can be further contacted with a superconductor (see the next section).

Electrical transport between a superconductor and a semiconductor is close to the subject of metal–semiconductor contacts. This has a long history, pretty much dominated by the subject of Schottky barriers. In this semiconductor-contact technology, the best one can achieve is an “ohmic” contact. It usually means that the IV curve is linear, and physically it is the regime where the Schottky barrier is thin enough, by high doping, to have a current only due to quantum mechanical tunneling through the Schottky barrier, without a thermally activated contribution. With a degenerately doped semiconductor, acting like a metal, and the normal-contact material in the superconducting state, it would act as a normal metal–insulator–superconductor (NIS), a Giaever-like tunnel junction. However, given the resistance per unit area for these contacts, the transmission probability T is very low, of the order of 10^{-4} , and therefore Andreev reflection would not contribute significantly to the current. Moreover, for silicon, for example, with a material like lead (Pb), it was found that the Schottky barrier is controlled not by the work function but rather by details of the atomic ordering at the interface (see, e.g., [101]). In practice, contact formation is usually mixed with complex materials issues. In the end, it has so far been impossible to obtain interesting physics with superconducting contacts on silicon or with GaAs/AlGaAs heterostructures, which were so successful for the quantum Hall effect and the quantum point contact. Instead, the most successful results have been obtained with InAs-based semiconductors. This material is unique because the surface states lead to an inversion layer at the top of the crystal, which provides an easily accessible 2-

dimensional electron gas. Currently, the interest in materials in which the surface acts as the conducting part has increased enormously.

In the study of ballistic Andreev reflections, the research with InAs-based heterostructures has provided at least one important experimental discovery. In semiconductor–superconductor contacts, at relatively low temperatures compared to T_c , a zero-bias anomaly, compared to the canonical BTK result, was first reported by Kastalsky et al. [102]. This anomaly consists of a peak in conductance centered around $V = 0$, which increases upon lowering the temperature. In subsequent work, it has become clear that it also occurs in normal-metal–superconductor systems and is not unique to semiconductors. However, transport in semiconductors is closer to ballistic, which led Van Wees et al. [103] to explain it in terms of ballistic Andreev reflection modified by the impurity scattering in front of the δ -function barrier introduced by Blonder et al. [14] for elastic scattering. Since the single-particle phase is conserved, it becomes possible that electrons are repeatedly scattered back, coherently, by the impurities to pass the δ -function barrier. This leads to the paradoxical behavior that adding impurity scattering enhances the Andreev reflection probability. In other words, this corrects for the deleterious effects of the Z parameter in Eq. (12).

In most of the remaining work on superconducting heterohybrids, the focus was on the interplay between single-particle phase-coherent transport, characteristic of the small scale of the normal metal, in interaction with the macroscopic phase of the superconductor. Since weak localization has a small effect and superconductivity a strong effect on the conductance, the dominating process is the effect of the superconductor on the normal metal, known as the proximity effect. By using multiply-connected devices, many experiments not possible before were carried out. An example is the study of phase-coherent normal transport controlled by scattering of electrons at different endings of a superconducting loop. In a SQUID-like fashion, the conductance becomes dependent on the macroscopic phase difference controlled with a magnetic field applied to the loop. This leads to oscillations in the conductance of a normal metal wire, and is often called Andreev interferometry, because it is understood as being due to the phase dependence of Andreev reflection. Some of these experiments were reviewed in 2004 in Ref. [104]. Most of the experiments are in the diffusive limit and only assume the Andreev reflection as the process through which the information of the macroscopic phase is communicated. The majority of

these experiments can be interpreted with the diffusive quasiclassical nonequilibrium theory [57]. Consequently, they shed very little direct light on the ballistic Andreev reflection process itself. But the advantage is that the experiments can be analyzed in many details in comparison to the well-developed diffusive theory. The best experimental system is a combination of a normal metal and a superconductor, rather than a semiconductor and a superconductor. A recent example is the work by Vercruyssen et al. [105], in which a superconducting nanowire was attached to two normal contacts at both ends. Instead of taking an old NS point contact configuration in the diffusive limit, a bulk N reservoir was connected to a superconducting wire, which was connected at the other end also to a large normal reservoir. This allows a one-dimensional analysis of the conversion of normal current to supercurrent, the evanescent states, another characteristic element of the Andreev reflection process taking place inside the superconductor, but in this case in the diffusive limit.

11. SUPERCONDUCTING NANOHYBRIDS: 1999–2002

Since about 1999, the progress in creating nano-objects, usually through a chemical route or “scotch tape”, has created a different type of superconducting nanostructures. They consist of bottom-up grown nano-objects, which can be found by inspection with an electron microscope, which also allows their local contact to electrical contacts. Although normal contacts provide an interesting range of phenomena, the use of superconductors as contacts contributes an extra energy and the phase-coherence condition. As expected, based on the universality of the Josephson effect, nano-objects used as a weak link between two superconductors carry a supercurrent with (depending on the geometry) some form of Fraunhofer-like response to a magnetic field and, often, the usual microwave-induced Shapiro steps. The experimentally and sometimes conceptually new aspect is that the nature of the nano-object and therefore the nature of the Josephson coupling can be tuned with a gate, which is also in competition with Coulomb interaction in these small structures. Since the coupling between the superconductor and the conductor plays a role, they are most often analyzed as quantum dots with superconducting leads. This has provided an interesting additional playground for model physics in which the effects of the spin (Kondo), the Coulomb blockade, and the Josephson coupling can be explored [106]. From an application

standpoint, a gateable Josephson junction is potentially of interest too. It can act as a three-terminal device, like the field-effect transistor, a possibility that has been lacking for many years and, as mentioned above, has hampered the development of the digital Josephson computer. However, with the new approaches, the gate voltages used are in the range of tens of volts, with an output voltage swing set by the $I_c R$ product, which is usually not much larger than a few tens of microvolts. Therefore, the gain of this type of transistor, a requirement for many practical applications, is absent. One of the few examples of a controllable Josephson junction, with an output voltage comparable to the input voltage, is the superconducting transistor demonstrated by Morpurgo et al. [107]. This particular transistor or controllable Josephson junction allows the control of the Josephson current by controlling the occupation of states in the weak link, either by hot electrons or by a nonequilibrium distribution [108, 109].

The field of superconducting nanohybrids is currently a very active field with high expectations and with a multitude of theoretical proposals, in particular, based on the new semiconducting nanowires. In the context of this overview, it is premature to draw a conclusion about the experimental status. It may be more useful to indicate what the experimental difficulties are to come to robust experimental data when working with superconducting nanohybrids. (Taken from Avouris et al. [110].)

12. EXPERIMENTAL COMPLEXITY OF SUPERCONDUCTING HYBRIDS

In the context of ballistic transport, superconducting heterohybrids and superconducting nanohybrids are experimentally difficult to control. As pointed out above, an attractive aspect of the GaAs/AlGaAs quantum point contacts and quantum dots in 2-dimensional electron gases and the mechanical break junctions is that they provide systems that perfectly satisfy the requirements of the Landauer–Büttiker scattering approach. The reservoirs are well-defined and clearly distinct from the scattering region, because of their larger volume, while at the same time they are made of the same material. This is also true for the superconducting atomic point contacts. The hybrids are, by definition, built from different materials. The reservoirs are made from a material that can become superconducting, to provide a source and a collector of electrons in the superconducting state. Since this result is achieved through a multi-step clean-room technology, the first

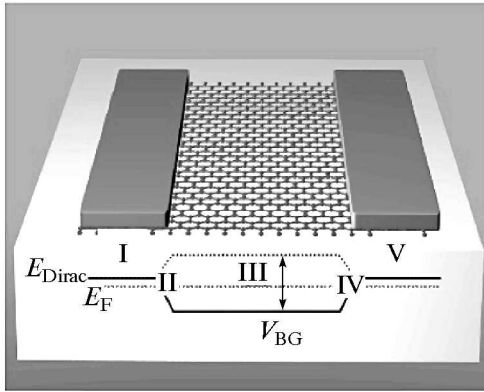


Fig. 12. An indication of the various domains that contribute to the quantum transport for graphene conductors with normal metal electrodes

question to be answered after fabrication of the device is what one has actually made. Usually, atoms forming the materials appear to be in the right spot, but this usually means not a lot from the point of view of the electrons. For semiconductor heterostructures, which are much more sensitive to dopants, the interfaces are made in UHV systems. For superconducting hybrids, such an *in situ* technology is not used and often not needed. Nevertheless, an important part of the experiments is the characterization of the device, usually by electrical transport, to determine what has actually been fabricated. Hence, the characterization of the devices by electrical measurements is intermixed with the identification of new physics and the choice of the best theoretical approach for the created nanostructure.

In many experiments with superconducting hybrids, a Josephson current is observed. However, a quantitative analysis turns out to be quite difficult. The observed critical current is usually smaller than expected, there is unaccounted hysteresis observed in the *IV* curves, there is often a lack of knowledge about the interface properties between the superconductor and the nano-object, and, finally, there is usually no quantitative analysis of the voltage-carrying state. To understand the transport processes in the superconducting hybrids better, we need a better understanding of the experimental system itself. The energy-dependent transport processes are the result of a mixture of elastic and Andreev reflection in a system in which ballistic and diffusive transport processes are distributed inhomogeneously.

The same level of uncertainty also occurs with normal electrodes. An example was recently provided by Avouris et al. [110]. In Fig. 12, a pictorial summary is

given of the regimes to be distinguished to understand short-channel graphene-based quantum coherent ballistic transport [110]. It has metal films of 20 nm Pd with 30 nm Au on top of graphene, with the graphene on SiO₂. Fabry–Perot resonances are observed for the electron branch of the *IV* curve, clearly signaling phase-coherent quantum transport. The length of the cavity is given by the uncovered part of the graphene, which indicates a reflection barrier at that interface, indicated by the Roman numeral II. In addition, a transmission coefficient T_{MG} between the metal and the graphene is identified, which is specified to be of the order of 0.4. The origin of this transmission coefficient is more systematically studied in Ref. [111]. In addition, the authors of [111] identified a gate-dependent transmission coefficient T_K , which is at the positions II. The main channel is area III, which is the channel that carries the Fabry–Perot resonances for the electrons. The absence of resonances for holes is attributed to the graphene underneath the metal being *p*-doped, meaning that the barrier in area II with T_K is the result of a *pn*- and an *np*-diode. Similarly, it is argued by Kretinin et al. [112] for their InAs wires coupled to Al electrodes that the relevant length for the Fabry–Perot resonances is at the edge of the metal-covered part and the uncovered part of InAs. And finally, the same has been found experimentally in carbon nanotubes by Liang et al. [113].

In most Josephson junction experiments, a similar search for the limiting experimental parameters is needed, because most experiments focus on the gateability of the Josephson current, and a Josephson current can be established through a complex barrier, whose details are not analyzed. An exception is in the work of Rohlfing et al. [114], where for a Nb–InAs Josephson contact for the transport channel, a transmission coefficient $T_{ch} = 0.8$ is found, whereas for the interface between the 2-dimensional electron gas in InAs and the superconducting metal the value $\tau_{NS} = 0.06$ is identified. Consequently, a high number of multiple Andreev reflections signal a highly transmissive conduction channel, but does not signal a highly transparent interface between the superconductor and the 2-dimensional electron gas.

At this point, it is worth returning to the experiments by Scheer et al. [98]. In this case, an atomic-scale contact of Au was used as the quantum conductor coupled to bilayers of Al and Au. By studying the contacts in the tunneling limit, they could measure the induced density of states in the N-part of the NS bilayer, which can be calculated using the Usadel theory and which has extensively been measured with tunnel junctions (in fact, it is the basis of the widely used niobium

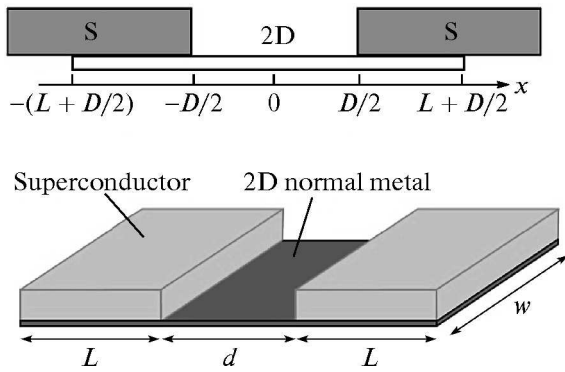


Fig. 13. A picture taken from [116] showing the finite dimensions that contribute to the proximity effect and therefore influence the energy-dependent conductance in a real device

trilayer-junction technology). Hence, they have very accurate information about the induced proximity effect in N. Subsequently, they brought the Au electrodes together, approaching the limit of highly transmissive channels. From a transmission-matrix point of view, the reservoirs are now formed by the induced proximity effect in N, which does not display a standard BCS form with just a lower gap but has the well-known features such as a strong peak at the edge of the spectral gap. This induced superconducting state is now the source and drain for the transmission matrix, with a proximity-induced Andreev reflection coefficient, also taking into account that a certain length of the gold is not covered by the superconductor. The results are shown in Fig. 11*b* with quite a good quantitative agreement, although not as good as in the full superconducting case in Fig. 11*a*.

Similarly, we can combine the insight obtained from the observations on the Fabry–Perot oscillations. They suggest that it is very plausible, depending on the details, that electron waves can also elastically scatter at the interface between the superconductor-covered and the uncovered part of graphene, a carbon nanotube or a semiconducting nanowire (region III in Fig. 12). And it is well known that a small amount of elastic scattering has a strong effect on the physical appearance of the *IV* curve. Consequently, the problem of a quantitative and conceptual understanding needs three different transmission coefficients: T_{NS} at the interface between the superconductor and the “normal” metal, T_E at the edge of the covered and the uncovered part, and the transmission coefficient T_{ch} of the actual quantum conductor (assuming that it is possible to split the system into a number of well-identified parts).

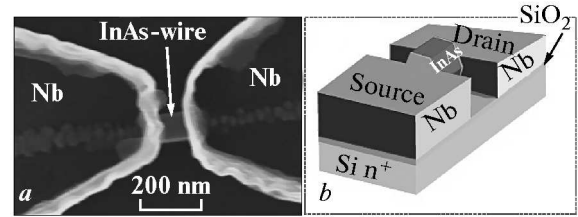


Fig. 14. An experimental attempt to create a better-defined contact between a superconductor and a semiconducting nanowire to reduce the number of unknown parameters and to create conditions for the electron waves, which are susceptible to a theoretical analysis. Figure taken from [118]

Finally, one more aspect of the problem is the superconductor itself. It is usually a thin film of finite length. Obviously, the metallic point contacts, which have served the field of point-contact spectroscopy very well, are providing massive equilibrium reservoirs. In thin-film microbridges, it was found important to make variable-thickness bridges in order to avoid thermal runaway at lower temperatures. These requirements were also needed in an experiment to study the two-point resistance of a superconducting wire between normal electrodes [105]. Apart from thermal equilibrium reservoirs, a finite-size superconductor is also contributing to the proximity effect (Fig. 13). This was addressed recently by Kopnin et al. [115, 116].

The process of Andreev reflection is indeed at the core of the transport properties of superconducting nanostructures, but it takes quite some effort for an experimentalist to find out exactly how. This is the main reason why the direct observation of the unique features of Andreev reflection is much more difficult in the modern-day nanostructures than in the old-fashioned point-contact technology and in point contact spectroscopy.

Two fruitful approaches can be used. One of them is to invest considerable experimental effort to disentangle all aspects of the problem. Along this path, the recent paper by Abay et al. [117] on InAs wires coupled to superconductors has made quite a bit of progress. The second approach is to simplify the experimental arrangement. An example is shown in Fig. 14, taken from [118]. A semiconductor nanowire is chopped off at the ends and the superconductor is attached at the tops. This should potentially reduce the number of relevant transmission coefficients. Similarly, such an approach has been used recently with a buried 2-dimensional electron gas by etching a mesa and attaching

the superconductor at the sides of the mesa, where it can reach the buried 2-dimensional electron gas [119], which allows a combination of ballistic transport in the 2-dimensional electron gas together with superconducting contacts, analogous to the Tsoi experiments, but with the added option of the interaction with the quantum Hall effect and/or the spin Hall effect.

A final example is an approach in which new reservoirs are constructed with special properties as a means to discover new physics in conventional materials. An example of this approach is provided by Khaire et al. [120], to demonstrate the triplet proximity effect. The commonly used approach to the proximity effect is based on singlet Cooper pairs, which is the standard interpretation of the Josephson current in an SNS system for a diffusive system. For a thin ferromagnetic layer between two superconductors, the Josephson coupling dies out rather quickly because of the large exchange energy in the ferromagnet, which leads to a very short coherence length. Khaire et al. placed two modified reservoirs of the singlet superconductor on both sides of the ferromagnet. Inspired by the work of Bergeret et al. [121], they modified the superconducting electrodes by covering them with a thin layer of normal metal followed by a very thin ferromagnet. This sandwich acted, through the thin ferromagnet, as a converter of singlet pairs into triplet pairs. They demonstrate that such triplet pairs have a long coherence length in a ferromagnet, in contrast to the singlet pairs. Although this experiment is performed in a diffusive system, it illustrates very nicely that a creative modification of the reservoir can considerably modify the transport, in this case, through a ferromagnet.

These examples illustrate that the superconducting hybrids are very interesting and rich in potential. Much more is to be expected, but they require very advanced material control and extensive characterization, which takes time. As we now see, time was also needed to directly measure the Andreev bound states predicted in 1965.

13. PHASE DEPENDENCE AND ANDREEV BOUND STATES: 1969, 1992, AND 2013

The last and very important characteristic of the Andreev reflection process is the dependence on the macroscopic quantum phase of the superconductor. The pair potential Δ appearing in Eq. (7) is a complex quantity with a well-defined phase ϕ . It becomes very relevant when phase coherence in a normal metal close to a superconductor is measured or when two super-

conductors are coupled through the process of Andreev reflection. The phase dependence is not emphasized in the original paper by Andreev [1]. It is also not very visibly present in a subsequent paper on the electronic states in the normal domains of a superconductor in the intermediate state. It is demonstrated that the energy levels are quantized [122]. This quantization is then used to calculate several thermodynamic quantities. In 1969, Kulik [22] addressed this phase dependence by pointing out that a bound state already assumes phase coherence, which, if the two superconductors have a different phase, makes the bound state energies dependent on the phase difference, leading to a discrete set of phase-dependent energies:

$$E_n^\pm = \frac{v_F}{2d} [2(\pi n + \alpha) \mp \phi], \quad (15)$$

where E_n is the n th energy level, v_F is the Fermi velocity, d is the thickness of the normal layer, n is an integer, and ϕ is the difference between the phases of the superconductors, $\phi_1 - \phi_2$. The quantity α is weakly energy-dependent, which becomes more relevant when E_n is closer to Δ_0 , the energy gap in the superconductor:

$$\alpha(E) = \arccos \frac{E}{\Delta_0}. \quad (16)$$

The levels E_n are twofold degenerate for $\phi = 0$ and split apart for $\phi \neq 0$, which is microscopically why there is a supercurrent running for a difference in the phases ϕ_1 and ϕ_2 , and the reason why there is a net Josephson current for $\phi \neq 0$. Kulik used this analysis to calculate the supercurrent in an SNS system, with a scattering free normal region. Beenakker and Van Houten [123] used the same approach for a one-dimensional model in which the normal domain is short compared to the coherence length. In that case, the thickness dependence disappears and the quantity α plays a key role, leading to a single twofold-degenerate Andreev level:

$$E_A = \pm \Delta \cos(\phi/2). \quad (17)$$

If there is scattering in the conduction channel with a transmission τ , the Andreev levels are given by

$$E_A = \pm \Delta \sqrt{1 - \tau \sin^2(\phi/2)}. \quad (18)$$

Ever since the first theoretical identification of discrete energy levels by Andreev and Kulik, several attempts have been made to measure these discrete levels directly by some form of spectroscopy. The lack of success until recently was partially because the requirement of one-dimensionality in a ballistic system was

not fulfilled in most experimental systems. The first indication was provided by Morpurgo et al. [124] by studying normal transport through a semi-ballistic coherent conductor of InAs of an InAs/AlSb heterostructure. The conductor was on both sides coupled to a superconductor connected in a loop. By applying a magnetic field, the phase difference on both sides of the conductor could be tuned, leading to the observation of a broad feature, which was consistent with an Andreev bound state. For a diffusive system, the supercurrent is carried not by a discrete set of states but by a continuum of states. This continuum of states also depends on the phase difference, as has been shown very clearly by Baselmans et al. [109] in creating a so-called π -junction by selectively populating the states in the N-part of an SNS junction. A full experimental observation of the discrete Andreev levels has been achieved only very recently. Pillet et al. [125] studied carbon nanotubes connected to superconductors at both ends. By attaching a third electrode to the middle of the nanotube, they were able to measure the individual states by quasiparticle injection spectroscopy. A very clear evolution of the individual states was observed, periodic in the phase difference, as expected from Eq. (17). A gate voltage was used to bring these quantum dot devices in the right regime for the observation of these Andreev bound states. Most recently, Bretheau et al. [126] used microwave spectroscopy in a mechanical break junction to probe the discrete levels and to occupy them selectively, with the finite transmission coefficients of the conduction channels in the atomic scale point contact, as contained in Eq. (18), taken into account. This work is, after many decades, the first experimental demonstration of the concept of phase-dependent Andreev bound states in a ballistic system, as first introduced by Kulik in 1969, and as a natural extension of the quantized levels introduced by Andreev in 1966.

14. CONCLUSIONS: 50 YEARS LATER

This review on the experimental proofs for the process called Andreev reflection leads to a somewhat surprising conclusion. The strongest evidence is provided by the experimental techniques based on point contacts developed prior to the modern era of nanotechnology. The more recent atomic-scale point contacts, which form a hybrid between the old-fashioned point-contact technique and thin-film technology, have also contributed very significantly to the quantitative evaluation of several aspects of

Andreev reflection. Such a quantitative evaluation has also been possible in many experiments based on diffusive inhomogeneous systems, in which the process of Andreev reflection is much more hidden and the theory is more complex. In the more recent semi-ballistic or partially ballistic thin-film-based superconducting hetero- and nanohybrids, the quantitative characterization of the electron transport is unfortunately less developed. And without the knowledge of the relevant experimental parameters, it is also more difficult to identify the most appropriate theoretical framework to interpret the results and to provide a quantitative evaluation. This ongoing research will undoubtedly continue for another decade or more. However, at this point in time, 50 years later, we can safely conclude that it has been an impressive *tour de force* to arrive at such an extremely fruitful concept as Andreev reflection inspired by the relatively “murky” experimental basis of the thermal conductivity of type-I superconductors in the intermediate state.

We thank A. V. Semenov, F. S. Bergeret, S. N. Artemenko and two anonymous referees for the critical reading of the manuscript and for providing helpful comments for improvement. Financial support from the Ministry of Education and Science of the Russian Federation under Contract No. 14.B25.31.0007 and from the European Research Council Advanced grant No. 339306 (METIQUIM) is gratefully acknowledged.

REFERENCES

1. A. F. Andreev, Zh. Eksp. Teor. Fiz. **46**, 1823 (1964) [Sov. Phys. JETP **19**, 1228 (1964)].
2. K. Mendelssohn and J. L. Olsen, Proc. Phys. Soc. (London) A **63**, 2 (1950); Phys. Rev. **80**, 859 (1950).
3. J. K. Hulm, Phys. Rev. **90**, 1116 (1953).
4. J. Bardeen, G. Rickayzen, and L. Tewordt, Phys. Rev. **113**, 982 (1959).
5. N. V. Zavaritskii, Zh. Eksp. Teor. Fiz. **38**, 1673 (1960) [Sov. Phys. JETP **11**, 1207 (1960)].
6. S. Strässler and P. Wyder, Phys. Rev. Lett. **10**, 225 (1963).
7. A. F. Andreev, Zh. Eksp. Teor. Fiz. **47**, 2222 (1964) [Sov. Phys. JETP **20**, 1490 (1964)].
8. V. L. Ginzburg and L. D. Landau, Zh. Eksp. Teor. Fiz. **20**, 1064 (1950).

9. J. Bardeen, L. N. Cooper, and J. R. Schrieffer, *Phys. Rev.* **106**, 162 (1957).
10. J. Bardeen, L. N. Cooper, and J. R. Schrieffer, *Phys. Rev.* **108**, 1175 (1957).
11. L. P. Gorkov, *Zh. Eksp. Teor. Fiz.* **34**, 735 (1958) [*Sov. Phys. JETP* **7**, 505 (1958)].
12. L. P. Gorkov, *Zh. Eksp. Teor. Fiz.* **36**, 1918 (1959) [*Sov. Phys. JETP* **9**, 1364 (1959)].
13. Yu. V. Sharvin, *Zh. Eksp. Teor. Fiz.* **48**, 984 (1965) [*Sov. Phys. JETP* **21**, 655 (1965)].
14. G. E. Blonder, M. Tinkham, and T. M. Klapwijk, *Phys. Rev. B* **25**, 4515 (1982).
15. R. Landauer, *IBM J. of Res. Dev.* **1**, 223 (1957).
16. M. Büttiker, Y. Imry, R. Landauer, and S. Pinhas, *Phys. Rev. B* **31**, 6207 (1985).
17. K. K. Likharev, *Rev. Mod. Phys.* **51**, 101 (1979).
18. L. G. Aslamazov and A. I. Larkin, *Pis'ma v Zh. Eksp. Teor. Fiz.* **9**, 150 (1969) [*Sov. Phys. JETP Lett.* **9**, 87 (1969)].
19. D. Saint-James, G. Sarma, and E. J. Thomas, *Type II Superconductivity*, Pergamon Press, Oxford (1969).
20. L. P. Gorkov, arXiv:1102.1098.
21. P. G. De Gennes and D. Saint-James, *Phys. Lett.* **4**, 151 (1963).
22. I. O. Kulik, *Zh. Eksp. Teor. Fiz.* **57**, 1745 (1969) [*Sov. Phys. JETP* **30**, 944 (1970)].
23. N. N. Bogoliubov, V. V. Tolmachov, and D. V. Shirkov, *Fortschritte der Physik* **6**, 605 (1958).
24. N. N. Bogoliubov, *Zh. Eksp. Teor. Fiz.* **34**, 58 (1958) [*Sov. Phys. JETP* **7**, 41 (1958)].
25. N. N. Bogoliubov, *Nuovo Cim.* **VII**, 794 (1958).
26. N. N. Bogoliubov, *Usp. Fiz. Nauk* **67**, 549 (1959) [*Sov. Phys. Uspekhi* **67**, 236 (1959)].
27. D. Saint-James, *J. de Phys.* **25**, 899 (1964).
28. P. G. de Gennes, *Superconductivity of Metals and Alloys*, W. A. Benjamin, New York (1966).
29. C. Caroli, P. G. de Gennes, and J. Matricon, *Phys. Lett.* **9**, 307 (1964).
30. D. V. Shirkov, arXiv:0903.3194.
31. G. Deutscher, *Rev. Mod. Phys.* **77**, 109 (2005).
32. A. F. Andreev, *Zh. Eksp. Teor. Fiz.* **49**, 655 (1966) [*Sov. Phys. JETP* **22**, 455 (1966)].
33. Yu. V. Sharvin and L. M. Fisher, *Pis'ma v Zh. Eksp. Teor. Fiz.* **1**(5), 54 (1965) [*JETP Lett.* **1**, 152 (1965)].
34. Yu. V. Sharvin and N. I. Bogatina, *Zh. Eksp. Teor. Fiz.* **56**, 772 (1969) [*Sov. Phys. JETP* **29**, 419 (1969)].
35. I. K. Yanson, *Zh. Eksp. Teor. Fiz.* **66**, 1035 (1974) [*Sov. Phys. JETP* **39**, 506 (1974)].
36. I. K. Yanson and Yu. N. Shalov, *Zh. Eksp. Teor. Fiz.* **71**, 286 (1976) [*Sov. Phys. JETP* **44**, 148 (1976)].
37. A. G. M. Jansen, F. M. Mueller, and P. Wyder, *Phys. Rev. B* **16**, 1325 (1977).
38. A. G. M. Jansen, F. M. Mueller, and P. Wyder, *Science* **199**, 1037 (1978).
39. V. S. Tsoi, *Pis'ma v Zh. Eksp. Teor. Fiz.* **19**, 114 (1974) [*JETP Lett.* **19**, 70 (1974)].
40. V. S. Tsoi, *Zh. Eksp. Teor. Fiz.* **68**, 1849 (1975) [*Sov. Phys. JETP* **41**, 927 (1975)].
41. V. S. Tsoi, J. Bass, P. A. M. Benistant, H. van Kempen, E. L. M. Payens, and P. Wyder, *J. Phys. F* **9**, L221 (1979).
42. A. H. Dayem and P. W. Anderson, *Phys. Rev. Lett.* **13**, 195 (1964).
43. J. E. Zimmerman and A. H. Silver, *Phys. Rev.* **141**, 367 (1966).
44. A. H. Dayem and C. C. Grimes, *Appl. Phys. Lett.* **9**, 47 (1966).
45. H. J. Levinstein and J. E. Kunzler, *Phys. Lett.* **20**, 581 (1966).
46. C. C. Grimes, P. L. Richards, and S. Shapiro, *Phys. Rev. Lett.* **17**, 431 (1966).
47. C. C. Grimes, P. L. Richards, and S. Shapiro, *J. Appl. Phys.* **39**, 3905 (1968).
48. A. Contaldo, *Rev. Sci. Instrum.* **38**, 1543 (1967).
49. W. C. Stewart, *Appl. Phys. Lett.* **12**, 277 (1968).
50. D. E. McCumber, *J. Appl. Phys.* **39**, 3113 (1968).
51. T. M. Klapwijk, M. Sepers, and J. E. Mooij, *J. Low Temp. Phys.* **27**, 801 (1977).
52. D. A. Weitz, W. J. Skocpol, and M. Tinkham, *Phys. Rev. Lett.* **40**, 253 (1978).
53. M. S. Khaikin and I. Ya. Krasnopolin, *Pis'ma v Zh. Eksp. Teor. Fiz.* **4**, 290 (1966).

54. A. F. Volkov and F. Ya. Nad', *Pis'ma v Zh. Eksp. Teor. Fiz.* **11**, 92 (1970).
55. A. N. Vystavkin, V. N. Gubankov, L. S. Kuzmin, K. K. Likharev, V. V. Migulin, and V. K. Semenov, *Revue de Physique Appliquée* **9**, 79 (1974).
56. N. B. Kopnin, *Theory of Nonequilibrium Superconductivity*, Oxford Univ. Press, Oxford (2001).
57. W. Belzig, F. K. Wilhelm, C. Bruder, G. Schön, and A. D. Zaikin, *Superlattices and Microstructures* **25**, 1251 (1999).
58. G. Eilenberger, *Z. Phys.* **214**, 195 (1968).
59. A. I. Larkin and Yu. N. Ovchinnikov, *Zh. Eksp. Teor. Fiz.* **55**, 2262 (1968) [*Sov. Phys. JETP* **26**, 1200 (1969)].
60. T. Matsubara, *Progr. Theor. Phys.* **14**, 351 (1955).
61. L. V. Keldysh, *Zh. Eksp. Theor. Phys.* **47**, 1515 (1964) [*Sov. Phys. JETP* **20**, 1018 (1965)].
62. A. Schmid and G. Schön, *J. Low Temp. Phys.* **20**, 207 (1975).
63. A. I. Larkin and Yu. N. Ovchinnikov, *Zh. Eksp. Teor. Fiz.* **68**, 1915 (1975) [*Sov. Phys. JETP* **41**, 960 (1975)].
64. A. I. Larkin and Yu. N. Ovchinnikov, *Zh. Eksp. Teor. Fiz.* **73**, 299 (1977) [*Sov. Phys. JETP* **46**, 155 (1977)].
65. A. A. Golub, *Zh. Eksp. Teor. Fiz.* **71**, 341 (1976) [*Sov. Phys. JETP* **44**, 178 (1976)].
66. L. G. Aslamazov and A. I. Larkin, *Zh. Eksp. Teor. Fiz.* **70**, 1340 (1976) [*Sov. Phys. JETP* **43**, 698 (1976)].
67. S. N. Artemenko, A. F. Volkov, and A. V. Zaitsev, *Zh. Eksp. Teor. Fiz.* **76**, 1816 (1979).
68. S. N. Artemenko, A. F. Volkov, and A. V. Zaitsev, *IEEE Trans. Magnetics* **MAG-15**, 471 (1979).
69. A. Schmid, G. Schön, and M. Tinkham, *Phys. Rev. B* **21**, 5076 (1980).
70. S. N. Artemenko, A. F. Volkov, and A. V. Zaitsev, *Pis'ma v Zh. Eksp. Teor. Fiz.* **28**, 637 (1978).
71. V. N. Gubankov and N. M. Margolin, *Pis'ma v Zh. Eksp. Teor. Fiz.* **29**, 733 (1979).
72. S. N. Artemenko, A. F. Volkov, and A. V. Zaitsev, *Sol. St. Comm.* **30**, 771 (1979).
73. S. N. Artemenko and A. F. Volkov, *Zh. Eksp. Teor. Fiz.* **72**, 1018 (1977) [*Sov. Phys. JETP* **45**, 533 (1977)].
74. A. G. Aronov and V. L. Gurevich, *Fiz. Tverd. Tela (Leningrad)* **16**, 1656 (1974) [*Sov. Phys. Solid State* **16**, 1722 (1974)].
75. T. M. Klapwijk, G. E. Blonder, and M. Tinkham, *Physica* **109&110B**, 1657 (1982).
76. J. Bardeen and J. L. Johnson, *Phys. Rev. B* **5**, 72 (1972).
77. M. Octavio, M. Tinkham, G. E. Blonder, and T. M. Klapwijk, *Phys. Rev. B* **27**, 6739 (1983).
78. A. V. Zaitsev, *Zh. Eksp. Teor. Fiz.* **78**, 221 (1980) [*Sov. Phys. JETP* **51**, 111 (1980)].
79. A. V. Zaitsev, *Zh. Eksp. Teor. Fiz.* **79**, 2016 (1980) Erratum [*Sov. Phys. JETP* **51**, 111 (1980) Erratum].
80. A. V. Zaitsev, *Zh. Eksp. Teor. Fiz.* **86**, 1742 (1984) [*Sov. Phys. JETP* **59**, 1015 (1984)].
81. G. E. Blonder and M. Tinkham, *Phys. Rev. B* **27**, 112 (1983).
82. G. Voss, PhD Thesis, *Statische und Dynamische Kennlinien von Metallischen Punktkontakten*, Cologne (1985).
83. L. Janson, M. Klein, H. Lewis, A. Lucas, A. Marantan, and K. Luna, *Amer. J. Phys.* **80**, 133 (2012).
84. W.-C. Lee, W. K. Park, H. Z. Arham, L. H. Greene, and P. W. Phillips, arXiv:1405.6357.
85. S. E. Bozhko, V. S. Tsoi, and S. E. Yakovlev, *Pis'ma v Zh. Eksp. Teor. Fiz.* **36**, 123 (1982) [*JETP Lett.* **36**, 153 (1983)].
86. P. A. M. Benistant, H. van Kempen, and P. Wyder, *Phys. Rev. Lett.* **51**, 817 (1983).
87. G. B. Lesovik and I. A. Sadovskyy, *Phys. Uspekhi* **54**, 1007 (2011).
88. R. Landauer, *Phil. Mag.* **21**, 863 (1970).
89. K. von Klitzing, G. Dorda, and M. Pepper, *Phys. Rev. Lett.* **45**, 494 (1980).
90. D. C. Tsui, H. L. Störmer, and A. C. Gossard, *Phys. Rev. Lett.* **48**, 1559 (1982).
91. P. C. van Son, H. van Kempen, and P. Wyder, *Phys. Rev. Lett.* **58**, 1567 (1987).
92. B. J. van Wees, H. van Houten, C. W. J. Beenakker, J. G. Williamson, L. P. Kouwenhoven, D. van der Marrel, and C. T. Foxon, *Phys. Rev. Lett.* **60**, 850 (1988).
93. H. van Houten, B. J. van Wees, J. E. Mooij, C. W. J. Beenakker, J. G. Williamson, and C. T. Foxon, *Europhys. Lett.* **5**, 721 (1988).
94. D. A. Wharam, T. J. Thornton, R. Newbury, M. Pepper, H. Ahmed, J. E. F. Frost, D. G. Hasko, D. C. Peacock, D. A. Ritchie, and G. A. C. Jones, *J. Phys. C* **21**, L209 (1988).

95. V. S. Tsoi, N. P. Tsoi, and S. E. Yakovlev, *Zh. Eksp. Teor. Fiz.* **95**, 921 (1989) [*Sov. Phys. JETP* **68**, 530 (1989)].
96. C. J. Muller, J. M. van Ruitenbeek, and L. J. de Jongh, *Physica C* **191**, 485 (1992).
97. E. Scheer, P. Joyez, D. Esteve, C. Urbina, and M. H. Devoret, *Phys. Rev. Lett.* **78**, 3535 (1997).
98. E. Scheer, W. Belzig, Y. Naveh, M. H. Devoret, D. Esteve, and C. Urbina, *Phys. Rev. Lett.* **86**, 284 (2001).
99. G. J. Dolan, *Appl. Phys. Lett.* **31**, 337 (1977).
100. L. N. Dunkleberger, *J. Vac. Sci. Technol.* **15**, 88 (1978).
101. D. R. Heslinga, H. H. Weitering, D. P. van der Werf, T. M. Klapwijk, and T. Hibma, *Phys. Rev. Lett.* **64**, 1589 (1990).
102. A. Kastalsky, A. W. Kleinsasser, L. H. Greene, R. Bhat, F. P. Milliken, and J. P. Harbison, *Phys. Rev. Lett.* **67**, 3026 (1991).
103. B. J. van Wees, P. de Vries, P. Magnée, and T. M. Klapwijk, *Phys. Rev. Lett.* **69**, 510 (1992).
104. T. M. Klapwijk, *J. of Superconductivity: Incorporating Novel Magnetism* **17**, 593 (2004).
105. N. Vercruyssen, T. G. A. Verhagen, M. G. Flokstra, J. P. Pekola, and T. M. Klapwijk, *Phys. Rev. B* **85**, 224503 (2012).
106. S. De Franceschi, L. P. Kouwenhoven, C. Schönberger, and W. Wernsdorfer, *Nature Nanotechnology* **5**, 703 (2010).
107. A. F. Morpurgo, T. M. Klapwijk, and B. J. van Wees, *Appl. Phys. Lett.* **72**, 966 (1998).
108. J. J. A. Baselmans, A. F. Morpurgo, B. J. van Wees, and T. M. Klapwijk, *Nature* **397**, 43 (1999).
109. J. J. A. Baselmans, T. T. Heikkilä, B. J. van Wees, and T. M. Klapwijk, *Phys. Rev. Lett.* **89**, 207002 (2002).
110. Yanqing Wu, Vasili Perebeinos, Yu-ming Lin, Tony Low, Fengnian Xia, and Phaedon Avouris, *NANO Lett.* **12**, 1417 (2012).
111. Fengnian Xia, Vasili Perebeinos, Yu-ming Lin, Yanqing Wu, and Phaedon Avouris, *Nature Nanotechnology* **6**, 179 (2011).
112. A. V. Kretinin, R. Popovitz-Biro, D. Mahalu, and H. Shtrikman, *NANO Lett.* **10**, 3439 (2010).
113. W. Liang, M. Bockrath, D. Bozovic, J. Hafner, M. Tinkham, and H. Park, *Nature* **411**, 665 (2001).
114. F. Rohlfing, G. Tkachov, F. Otto, K. Richter, D. Weiss, G. Borghs, and C. Strunk, *Phys. Rev. B* **80**, 220507(R) (2009).
115. N. B. Kopnin and A. S. Mel'nikov, *Phys. Rev. B* **84**, 064524 (2011).
116. N. B. Kopnin, A. S. Melnikov, I. A. Sadovskyy, and V. M. Vinokur, *Phys. Rev. B* **89**, 081402(R) (2014).
117. S. Abay, D. Persson, H. Nilsson, F. Wu, H. Q. Xu, M. Fogelström, V. Shumeiko, and Per Delsing, arXiv:1311.1745 (cond-mat).
118. H. Y. Günel, *Quantum Transport in Nanowire-Based Hybrid Devices*, MSc Thesis, TU Aachen (2013).
119. A. Kononov, N. Titova, G. Biasiol, L. Sorba, and E. V. Deviatov, arXiv:1305.5685 (cond-mat).
120. T. S. Khaire, M. A. Khasawneh, W. P. Pratt Jr., and N. O. Birge, *Phys. Rev. Lett.* **104**, 137002 (2010).
121. F. S. Bergeret, A. F. Volkov, and K. B. Efetov, *Rev. Mod. Phys.* **77**, 1321 (2005).
122. A. F. Andreev, *Zh. Eksp. Teor. Fiz.* **49**, 655 (1964) [*Sov. Phys. JETP* **22**, 455 (1966)].
123. C. W. J. Beenakker and H. van Houten, *Phys. Rev. Lett.* **66**, 3056 (1991).
124. A. F. Morpurgo, B. J. van Wees, T. M. Klapwijk, and G. Borghs, *Phys. Rev. Lett.* **79**, 4010 (1997).
125. J.-D. Pillet, C. H. L. Quay, P. Morfin, C. Bena, A. Levy Yeyati, and P. Joyez, *Nat. Phys.* **6**, 965969 (2010).
126. L. Bretheau, C. Ö. Girit, H. Pothier, D. Estève, and C. Urbina, *Nature* **499**, 312 (2013).